Article

Analytical modeling of the temporal evolution of epidemics outbreaks accounting for vaccinations

Reinhard Schlickeiser [1,2]* and Martin Kröger [3]*

[1] Institut für Theoretische Physik, Lehrstuhl IV: Weltraum- und Astrophysik, Ruhr-Universität Bochum, D-44780 Bochum, Germany
[2] Institut für Theoretische Physik und Astrophysik, Christian-Albrechts-Universität zu Kiel, Leibnizstr. 15, D-24118 Kiel, Germany
[3] Polymer Physics, Department of Materials, ETH Zurich, Zurich CH-8093, Switzerland
* Correspondence: rsch@tp4.rub.de (R.S.); mk@mat.ethz.ch (M.K.)

Abstract: With the now available vaccination against Covid-19 it is quantitatively explored how vaccination campaigns influence the mathematical modeling of epidemics. The standard susceptible-infectious-recovered/removed (SIR) epidemic model is extended to the fourth compartment V of vaccinated persons and the vaccination rate $v(t)$ that regulates the relation between susceptible and vaccinated persons. The vaccination rate $v(t)$ competes with the infection ($a(t)$) and recovery ($\mu(t)$) rates in determining the time evolution of epidemics. In order for a pandemic outburst with rising rates of new infections it is required that $k + b < 1 - 2\eta$, where $k = \mu_0/a_0$ and $b = v_0/a_0$ denote the initial ratios of the three rates, respectively, and $\eta \ll 1$ is the initial fraction of infected persons. Exact analytical inverse solutions $t(Q)$ for all relevant quantities $Q = [S, I, R, V]$ of the resulting SIRV-model in terms of Lambert functions are derived for the semi-time case with time-independent ratios k and b between the recovery and vaccination rates to the infection rate, respectively. These inverse solutions can be approximated with high accuracy yielding the explicit time-dependences Q(t) by inverting the Lambert functions. The values of the three parameters k, b and η completely determine the reduced time evolution the SIRV-quantities $Q(\tau)$. The influence of vaccinations on the total cumulative number and the maximum rate of new infections in different countries is calculated by comparing with monitored real time Covid-19 data. The reduction in the final cumulative fraction of infected persons and in the maximum daily rate of new infections is quantitatively determined by using the actual pandemic parameters in different countries. Moreover, a new criterion is developed that decides on the occurrence of future Covid-19 waves in these countries. Apart from Israel this can happen in all countries considered.

Keywords: coronavirus; statistical analysis; extrapolation; parameter estimation; pandemic spreading

Citation: Schlickeiser, R.; Kröger, M. Analytical modeling of the temporal evolution of epidemics outbreaks accounting for vaccinations. *Preprints* **2021**, *1*, 0. https://doi.org/

Received: 2021-03-28
Accepted:
Published:

1. Introduction

In December 2020 the effective mRNA-based Covid-19 vaccine by the companies Pfizer-BioNTech and Moderna became available. This has lead to intensive vaccination campaigns in many countries over the world with different speeds. As two shots per person are needed for nearly 100 percent protection as of February 10, 2021, Israel with a time t-dependent vaccination rate of $v(t) \simeq 7.0 \times 10^{-3}$ day^{-1} has the highest, followed by the United Arab Emirates $v(t) \simeq 4.7 \times 10^{-3}$ day^{-1}, United Kingdom with $v(t) \simeq 2.0 \times 10^{-3}$ day^{-1}, whereas Germany's vaccination rate $v(t) \simeq 4.2 \times 10^{-4}$ day^{-1} is significantly smaller.

It is the purpose of the present manuscript to investigate analytically and quantitatively for a given ratio $b(t) = v(t)/a(t)$ of the vaccination rate to infection rate $a(t)$ the effect on the time evolution of the ongoing epidemic waves. We base the analysis on the susceptible-infectious-recovered/removed (SIR) epidemic model [1] augmented by the appropriate vaccination rates leading to the susceptible-infectious-recovered/removed-vaccinated (SIRV) epidemic model. This model is a dynamical system for time-dependent quantities $S(t)$, $I(t)$, $R(t)$ and $V(t)$ denoting the relative fractions of currently susceptible (S), infectious (I), recovered/removed (R) and vaccinated (V) persons in the considered

Preprints (www.preprints.org) | NOT PEER-REVIEWED | Posted: 30 March 2021 doi:10.20944/preprints202103.0718.v1

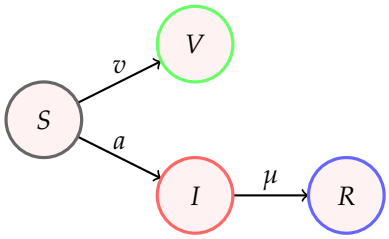

Figure 1. The three time-dependent rates $a(t)$, $\mu(t)$, and $v(t)$ entering the SIRV equations for the four compartments of susceptible (S), infectious (I), recovered (R), and vaccinated (V) population fractions. Upon introducing reduced time τ, the model is characterized by the assumed constant ratios $k = \mu(t)/a(t)$ and $b = v(t)/a(t)$.

population of N persons as a function of time t (Fig. 1). In the case of negligible vaccination, assuming a constant ratio between infection and recovery rate, considerable improvements on the analytical modelling of epidemics with this compartment model has been achieved citeks20,sk21. We make frequent use of these improvements in the following.

Application of this earlier work [2] to the monitored second waves in many countries has indicated initial infection rates of the order of $a(0) \in [0.1\text{–}1.0]$ day^{-1}, considerably greater than the above vaccination rates. However, it is important to emphasize an essential difference: whereas the initial vaccination and the recovery rate can be directly used to estimate the corresponding typical time scales $T_v \simeq 1/v(0)$ and $T_r \simeq 1/\mu(0)$ for vaccinations and recovery, respectively, the initial infection time scale $T_i = 1/[a(0)I(0)]$ additionally depends on the initial fraction $I(0)$ of infected persons at the onset of the 2nd wave. With this, and depending on the country, the vaccination time scale T_v is often comparable with the infection time scale T_i.

The inferred infection rates are slightly larger than the initial recovery rates $\mu(0)$ so that the ratio of the two $k = \mu(0)/a(0) \in [0.8, 1)$. This is consistent with the result [3] that for a pandemic outburst with a prominent peak at a later time the ratio k has to be smaller than $k < 1 - 2\eta$, where $\eta = I(0)$ is used. For most second waves $\eta \ll 1$ is negligibly small, so that the determined values of k less than unity are fully consistent. Then with the above noted vaccination rates the ratio of the vaccination to initial recovery rates $b = v(t)/\mu(0)$ is considerably smaller than the ratio k: we expect values of $b \in [5 \times 10^{-4}, 10^{-2}] \ll k$. Consequently, the difference $\alpha = k - b$ is positive and only slightly smaller than k. We may refer to α as the effective ratio as compared to the ratio k.

It is the purpose of this manuscript to determine quantitatively the influence of this small reduction of the ratio k on the time evolution of the pandemic wave. As in earlier work before our analytical calculations are based on the assumption that the ratios k and b are constants; but they hold for arbitrary time dependent infection rates $a(t)$, where, however, the recovery and vaccination rate follow the very same time dependence as $a(t)$.

Compartment models for epidemics with vaccinations have been considered before [4–7] but they were more concerned with optimizing the control of the epidemics by vaccination with limited resources. Our main goal of this study is to derive analytical solutions for the dynamical SIRV to be presented in Eqs. (1)–(5). In order to keep the analysis as simple and transparent as possible we ignore complicating issues such as age grouping, vital dynamics and/or spatial spread effects that have been recently investigated in the literature [8,9] with numerical solutions.

2. General SIRV equations

The SIRV-model is a dynamical system for time-dependent population fractions $S(t)$, $I(t)$, $R(t)$ and $V(t)$ introduced above. The fractions add up to unity, $S(t) + I(t) + R(t) +$

 doi:10.20944/preprints202103.0718.v1

$V(t) = 1$ at all times (sum constraint). The SIRV differential equations accounting for vaccinations of the susceptible persons with the vaccination rate $v(t)$ read

$$\dot{S} = -a(t)SI - v(t)S, \quad (1)$$
$$\dot{I} = a(t)SI - \mu(t)I, \quad (2)$$
$$\dot{R} = \mu(t)I, \quad (3)$$
$$\dot{V} = v(t)S, \quad (4)$$

where the dot denotes a derivative with respect to time t. The SIRV equations are supplemented by semi-time initial conditions (defining $t = 0$)

$$S(0) = 1 - \eta, \quad I(0) = \eta, \quad R(0) = V(0) = 0 \quad (5)$$

with $\eta \in (0, 1)$ denoting the fraction of infected persons at time $t = 0$. One of the four dynamical equations can also be replaced by the sum constraint.

These initial conditions are sufficient to capture applications of the SIRV equations with non-vanishing $R(0)$ and $V(0)$ as this is identical with the present initial condition upon subtracting the nonvanishing $\Delta N = N[R(0) + V(0)]$ from N. The resulting SIRV quantities are then fractions of the reduced, susceptible or currently infected population, and the fractions S and I with respect to the total population N are obtained by multiplying them both with $1 - (\Delta N/N)$. Similarly, the total number of recovered and vaccinated persons is $(N - \Delta N)R$ plus $NR(0)$, same for V. More formally, if $\tilde{X}$ denotes one of the SIRV quantities that fulfills initial condition $\tilde{X}(0)$, the time-evolution of $\tilde{X}$ is given by the time-evolution of X via $\tilde{X} = \chi X$ for $X \in \{S, I\}$ and $\tilde{X} = \tilde{X}(0) + \chi X$ for $X \in \{R, V\}$ with $\chi = \tilde{I}(0) + \tilde{S}(0)$.

The initial conditions (5) are specified by $\tilde{\eta} = \tilde{I}(0)/\chi$, and the parameters to be introduced next have to be adjusted as well, $\tilde{k} = \chi k$ and $\tilde{b} = \chi b$.

The fractions $S(t)$, $I(t)$, and $R(t)$ are usually not measurable with high confidence, while the daily new number of infected persons, denoted by

$$\dot{J} = a(t)SI, \quad (6)$$

and the fraction of vaccinated persons, $V(t)$, are two quantities that can be more easily measured, and are usually reported. Using Eqs. (1) and (4) the total cumulative number fraction J of persons, that have been infected up to the time t, is related to the SIRV quantities via

$$J(t) = \int_{-\infty}^{t} \dot{J}(\xi) d\xi = 1 - S(t) - V(t) \quad (7)$$

or equivalently, upon making use of the sum constraint, by the sum of currently infected and currently recovered, $J(t) = I(t) + R(t)$.

Following previous works, and to make sure that the SIRV model has any predictive power, we will allow for arbitrary time-dependent rate $a(t)$ throughout this work, but assume at the same time that the remaining rates $\mu(t)$ and $v(t)$ exhibit the identical dependency with respect to time. This leaves us with two time-independent model parameters,

$$k = \frac{\mu(t)}{a(t)}, \qquad b = \frac{v(t)}{a(t)} \quad (8)$$

As we will demonstrate the two parameters k and b together with the initial fraction of infected persons η completely determine the temporal evolution of the pandemic wave in the reduced time $\tau = \int_0^t d\xi a(\xi)$.

Preprints (www.preprints.org) | NOT PEER-REVIEWED | Posted: 30 March 2021 doi:10.20944/preprints202103.0718.v1

2.1. Condition for pandemic outburst

It is instructive to calculate with the first two SIRV equations the initial variation of the daily number of the newly infected population fraction,

$$\begin{aligned} \ddot{J} &= \dot{a}SI + a(I\dot{S} + S\dot{I}) \\ &= \dot{J}[\dot{a}/a + a(S-I) - \mu - v] \\ &= \dot{J}\{\dot{a}/a + a[(S-I) - k - b]\} \end{aligned} \tag{9}$$

where we have omitted the argument t for all functions, and used Eq. (8). In order for a pandemic outburst with initially rising rates of new infections $\ddot{J}(0) > 0$ to occur the bracket on the right-hand side of Eq. (9) has to be positive at the starting time $t = 0$, so that with initially constant rate values $\dot{a}(0) = 0$ it is required that $[(S(0) - I(0)] - k - b > 0$. Making use of the first two initial conditions (5) the outburst condition reads

$$k + b < 1 - 2\eta \tag{10}$$

As k and b have positive values the condition (10) implies:

(i) If initially more than 50 percent ($\eta > 0.5$) are infectious, no new pandemic outburst will occur. However, such high values of η are unlikely and unrealistic.

(ii) For small given values of $\eta \ll 0.5$ and the ratio of recovered to infection rate k, new emerging outbreaks can be fully prevented for values of the ratio of vaccination to infection rate $b > 1 - k - 2\eta \simeq 1 - k$. The more pathogenic a virus mutation is, the smaller and closer to zero is the value of the ratio k so that the lower limit for b has to be close to unity to prevent a new outburst.

(iii) For any finite value of η for modeling epidemic outbreaks the relevant range of the two parameters k and b is $0 \leq b + k < 1$.

(iv) As an aside we note that Eq. (10) demonstrates that in the SIR-model with $b = 0$ no pandemic wave can occur if the parameter $k = 1$ equals unity. The SIR-model correctly indicates that epidemic waves end in the case $k = 1$. Therefore the recent criticism [10] on the SIR-model is inappropriate and misguided.

2.2. Reduced time

We consider the case where the ratios of the recovery to infection rate, $\mu(t)/a(t) = k$, and the vaccination to infection rate, $v(t)/a(t) = b$, are semipositive constants independent of time. This assumption still allows us to account for any given time-dependence of the infection rate with the caveat that the recovery and vaccination rate have exactly the same time dependence as the infection rate apart from their different initial values. The introduction of the reduced time scale

$$\tau = \int_0^t d\xi\, a(\xi) \tag{11}$$

reduces the SIRV equations (1) - (4) to

$$\frac{dS}{d\tau} = -SI - bS, \tag{12}$$

$$\frac{dI}{d\tau} = SI - kI, \tag{13}$$

$$\frac{dR}{d\tau} = kI, \tag{14}$$

$$\frac{dV}{d\tau} = bS, \tag{15}$$

Eqs. (12) and (13) readily yield

Preprints (www.preprints.org) | NOT PEER-REVIEWED | Posted: 30 March 2021 doi:10.20944/preprints202103.0718.v1

$$I = -[b + \frac{d\ln S}{d\tau}], \tag{16}$$
$$S = k + \frac{d\ln I}{d\tau}, \tag{17}$$

providing for Eqs. (14) and (15)

$$\frac{d}{d\tau}[R + k\ln S + bk\tau] = 0, \tag{18}$$
$$\frac{d}{d\tau}[V - b\ln I - bk\tau] = 0. \tag{19}$$

Both equations integrate immediately to

$$R(\tau) = -k\ln S(\tau) + k\ln(1-\eta) - bk\tau, \tag{20}$$
$$V(\tau) = b\ln I(\tau) - b\ln\eta + bk\tau, \tag{21}$$

where the integration constants have been determined with the initial conditions (5) holding now at $\tau = 0$. In terms of the reduced time τ the differential new number of infected persons $j(\tau) = dJ(\tau)/d\tau = \dot{J}(t)/a(t)$ is

$$j(\tau) = \frac{dJ(\tau)}{d\tau} = S(\tau)I(\tau) \tag{22}$$

while the corresponding cumulative fraction is

$$J(\tau) = \int_{-\infty}^{\tau} j(\tau')d\tau' = 1 - S(\tau) - V(\tau) = I(\tau) + R(\tau) \tag{23}$$

At $\tau = 0$, the cumulative $J(0) = I(0) + R(0) = \eta$. In reduced time Eq. (9) corresponds to

$$\frac{1}{j}\frac{dj}{d\tau} = \frac{d\ln j}{d\tau} = S(\tau) - I(\tau) - k - b \tag{24}$$

We have so far expressed R, V, J, and j in terms of S and I. An additional relationship between S and I is provided by the sum constraint, as shown next, and this will allow us to come up with a closed equation for a single variable, to be developed in the next section.

Inserting Eqs. (16)–(17), (20) and (21) provides for the sum constraint

$$\frac{d\ln I}{d\tau} - \frac{d\ln S}{d\tau} + b\ln I - k\ln S = 1 + b - k + b\ln\eta - k\ln(1-\eta) \tag{25}$$
$$= 1 + (b-k)[1 + \ln\eta(1-\eta)] + k\ln\eta - b\ln(1-\eta)$$

In the present manuscript we will derive analytical solutions of Eq. (25) for general non-zero and different values of $b \neq k$. We will obtain an implicit analytic solution that expresses the reduced τ in terms of a parameter ψ, while all SIRV-functions including j are expressed in this parameter. We further present a highly accurate analytical approximation for all SIRV-functions as a function of τ. Our new analytical solutions reduce in the appropriate limit to the earlier [2,3,11] solutions for the non-vaccination case $b = 0$. We also consider as special cases the non-recovery case $k = 0$ and the special case of equal values of $k = b$.

3. Dynamics of the epidemics

3.1. Summary of results

Because the following derivation of the solution of the SIRV equations (11)-(15) in reduced time with parameters k and b, and subject to initial conditions $I(0) = 1 - S(0) = \eta$ and $R(0) = V(0)$ is rather lengthy, we begin by stating the final result. We are able to derive an implicit exact solution $\tau = \tau(\psi)$ parameterized by ψ, while all SIRV quantities can be expressed in ψ as well. Provided the reduced vaccination rate b exceeds a critical b_c,

Preprints (www.preprints.org) | NOT PEER-REVIEWED | Posted: 30 March 2021 doi:10.20944/preprints202103.0718.v1

for which we provide the explicit expression (91), we show that the explicit solution of the SIRV equation can be written as follows. With the help of $\psi(\tau) = \ln[S(\tau)/I(\tau)]$,

$$\psi(\tau) = \ln\frac{1-\eta}{\eta} + (k-b)\tau - \frac{1-e^{-b\tau}}{b} \tag{26}$$

we obtain

$$S(\tau) = \frac{e^{-b\tau}}{1+e^{-\psi(\tau)}}, \qquad I(\tau) = \frac{e^{-b\tau}}{1+e^{\psi(\tau)}} \tag{27}$$

$$R(\tau) = J(\tau) - I(\tau), \qquad V(\tau) = 1 - S(\tau) - J(\tau) \tag{28}$$

where the differential j and cumulative fractions J of infected persons are given by

$$j(\tau) = S(\tau)I(\tau), \tag{29}$$

$$J(\tau) = \eta + \int_0^\tau j(\tau')d\tau'. \tag{30}$$

If b is smaller than the critical b_c, provided by Eq. (91), the SIRV model approaches the SIR model that has been treated before, and the SIRV quantities are well captured by a simple linear superposition of the SIR result with the above SIRV solution evaluated at $b = b_c$. Next we derive these expressions and provide additional features of the solution such as the final values at $t \to \infty$, treat special cases such as $k = b$, and discuss the features of the SIRV equations that gave rise to Eq. (26). The solution holds for any semipositive values of k and b.

3.2. Two useful functions

We start the mathematical analysis by introducing the function

$$\psi(\tau) = \ln\frac{S(\tau)}{I(\tau)}, \tag{31}$$

implying

$$I(\tau) = S(\tau)e^{-\psi(\tau)} \tag{32}$$

with the usually positive (for initial fractions $\eta < 0.5$ of infected persons) initial value

$$\psi_0 \equiv \psi(\tau = 0) = \ln\frac{1-\eta}{\eta} \tag{33}$$

The first derivative of the ψ (31) is given by

$$\frac{d\psi}{d\tau} = \frac{I\frac{dS}{d\tau} - S\frac{dI}{d\tau}}{IS} = \alpha - (I+S), \tag{34}$$

where we used Eqs. (12) and (13) and where the following abbreviation is introduced

$$\alpha = k - b \tag{35}$$

Consequently, the function

$$\Phi(\tau) = \alpha - \frac{d\psi}{d\tau} = I(\tau) + S(\tau), \tag{36}$$

is always positive and has values $\Phi \in [0,1]$ as I and S are positively valued fractions at all times.

Equation (21) is identical to $I(\tau) = \eta\exp[-k\tau - (V(\tau)/b)]$, and since $k > 0$ and with V residing in the finite interval $[0,1]$ we find that after infinite time $I_\infty = I(\tau = \infty) = 0$.

Preprints (www.preprints.org) | NOT PEER-REVIEWED | Posted: 30 March 2021 doi:10.20944/preprints202103.0718.v1

Similarly, Eq. (20) is identical with $S(\tau) = (1-\eta)\exp[-b\tau - R(\tau)/k]$, so that with $b > 0$ and R residing in the finite interval $[0,1]$, one has $S_\infty = S(\tau = \infty) = 0$. Consequently, $\Phi_\infty = 0$ ultimately vanishes as well. In this limit Eq. (36) says that $d\psi/d\tau$ is reaching the constant α, and thus $\psi_\infty = \psi(\tau = \infty) = \text{sign}(\alpha)\infty$ is infinitely large, while its sign is given by the sign of α, as long as $\alpha \neq 0$. For $\alpha = 0$ the ψ_∞ reaches a constant value.

The initial slope of $d\psi/d\tau$ evaluates to

$$\left.\frac{d\psi}{d\tau}\right|_{\tau=0} = -(1-\alpha) \tag{37}$$

and is thus negative for all $\alpha = k - b < 1$ and positive for $\alpha > 1$. This implies, that the function ψ decreases initially, undergoes a minimum ψ_m at $\Phi_m = \alpha$ before increasing to its final value $\psi_\infty = \infty$, when $\alpha \in (0,1)$. For negative α, ψ monotonously decreases, while for $\alpha > 1$ the ψ monotonously increases.

For all non-zero values of k and b the function $\Phi = I + S$, however, decreases at all times from its initial maximum value $\Phi(0) = 1$ as its derivative is always seminegative, i.e.

$$\frac{d\Phi}{d\tau} = \frac{dI}{d\tau} + \frac{dS}{d\tau} = -(bS + kI), \tag{38}$$

where we again used Eqs. (12) and (13).

3.3. Mathematical analysis

With Eq. (32) the two Eqs. (36) and (38) yield

$$\Phi = S(1 + e^{-\psi}), \qquad \frac{d\Phi}{d\tau} = -S(b + ke^{-\psi}) \tag{39}$$

The combination of these two Eqs. (39) then provides

$$\frac{d\Phi}{d\tau} = -\Phi\left[\frac{b + ke^{-\psi}}{1 + e^{-\psi}}\right] \tag{40}$$

or equivalently,

$$\frac{d\ln\Phi}{d\tau} + A(\psi) = 0 \tag{41}$$

with the function

$$A(\psi) = \frac{b}{1 + e^{-\psi}} + \frac{k}{1 + e^{\psi}} = \frac{dB(\psi)}{d\psi}, \tag{42}$$

which we prefer to write as the derivative of B given by

$$B(\psi) = b\ln(1 + e^{\psi}) - k\ln(1 + e^{-\psi}) = k\psi - \alpha\ln(1 + e^{\psi}) \tag{43}$$

With the function (43) we obtain for Eq. (41) multiplied with $(d\psi/d\tau) = \alpha - \Phi$ from Eq. (36)

$$\begin{aligned}(\Phi - \alpha)\frac{d\ln\Phi}{d\tau} - \frac{d\psi}{d\tau}\frac{dB}{d\psi} &= \Phi\frac{d\ln\Phi}{d\tau} - \alpha\frac{d\ln\Phi}{d\tau} - \frac{dB}{d\tau} \\ &= \frac{d\Phi}{d\tau} - \alpha\frac{d\ln\Phi}{d\tau} - \frac{dB}{d\tau} \\ &= \frac{d}{d\tau}[\Phi - \alpha\ln\Phi - B] = 0\end{aligned} \tag{44}$$

with the first integral

$$c_0 = \Phi - \alpha\ln\Phi - B(\psi) = 1 - B(0), \tag{45}$$

where the integration constant $c_0 = 1 - B(0)$ is fixed by the initial conditions $\Phi(0) = 1$. Equation (45) then becomes

Preprints (www.preprints.org) | NOT PEER-REVIEWED | Posted: 30 March 2021 doi:10.20944/preprints202103.0718.v1

$$\Phi - \alpha \ln \Phi = 1 + k(\psi - \psi_0) - \alpha \ln[\eta(1 + e^{\psi})], \tag{46}$$

which is the first important result of this study. Together with Eq. (36) we can identify firstly, the relation to earlier obtained solutions for special values of b and k, and secondly derive the general solution for the epidemic time evolution for general values of b and k. When the time dependence of $\Phi(\tau)$ and $\psi(\tau)$ according to Eqs. (46) with (36) has been inferred, then acccording to Eqs. (32) and (39) we obtain

$$S(\tau) = \frac{\Phi(\tau)}{1 + e^{-\psi}} = \frac{\alpha - \frac{d\psi}{d\tau}}{1 + e^{-\psi}}, \tag{47}$$

$$I(\tau) = \frac{\Phi(\tau)}{1 + e^{\psi}} = \frac{\alpha - \frac{d\psi}{d\tau}}{1 + e^{\psi}} \tag{48}$$

while the remaining $R(\tau)$ and $V(\tau)$ were already expressed in terms of $S(\tau)$ and $I(\tau)$ in Eqs. (20) - (21), so that

$$R(\tau) = -bk\tau - k \ln \Phi(\tau) + k \ln[(1 - \eta)(1 + e^{-\psi})], \tag{49}$$

$$V(\tau) = bk\tau + b \ln \Phi(\tau) - b \ln[\eta(1 + e^{\psi})] \tag{50}$$

3.4. Inverse solution for the general case

In the general case $b \neq k$ the transcendental Eq. (46) is solved in terms of the real-valued Lambert functions [11]. We discuss below which of the two existing real-valued Lambert functions W_0 (principal) and W_{-1} (non-principal), respectively, applies in different parameter ranges. For the moment the notation W without an index represents both alternatives.

As $\Phi \leq 1$ we set $\Phi = e^{-x}$ with non-negative values of x to find for Eq. (46) the so-called Lambert equation

$$e^{-x} = -\alpha(x - r), \tag{51}$$

with

$$r = \frac{1 + k(\psi - \psi_0)}{\alpha} - \ln[\eta(1 + e^{\psi})] \tag{52}$$

The transcendental Eq. (51) has the solution [11]

$$x = r + W(-\frac{e^{-r}}{\alpha}), \tag{53}$$

so that

$$\Phi = e^{-r - W(-\frac{e^{-r}}{\alpha})} = -\alpha W\left(-\frac{e^{-r}}{\alpha}\right), \tag{54}$$

where we used the identity $e^{-aW(z)} = [W(z)/z]^a$ with $a = 1$ here. Using r from Eq. (52) we finally find the exact relationship between Φ and ψ as

$$\Phi = -\alpha W\left(-\frac{E(\psi)}{\alpha}\right), \tag{55}$$

with the positive expression

$$E(\psi) = \eta(1 + e^{\psi}) e^{-\frac{[1 + k(\psi - \psi_0)]}{\alpha}} \geq 0, \tag{56}$$

We emphasize that E is nonnegative irrespective of the sign of α. At time $\tau = 0$, E evaluates to $E(\psi_0) = e^{-1/\alpha}$. We had already proven that ψ asymptotically reaches $\text{sign}(\alpha)\infty$. This implies $E_\infty = \lim_{\tau \to \infty} \eta[e^{\psi(1-k)/\alpha)}]$. Because $\alpha < k$ and $k > 0$ in general, the $(1 - k)/\alpha$ has the sign of $-\alpha$, and $E_\infty = 0$ for any $\alpha \neq 0$. Further, because the derivative of $E(\psi)$ with

Preprints (www.preprints.org) | NOT PEER-REVIEWED | Posted: 30 March 2021 doi:10.20944/preprints202103.0718.v1

respect to ψ vanishes only at $\psi = \ln(-k/b)$, and thus nowhere for positive k and b, the $E(\psi)$ has no extremum with respect to ψ. For the same reason E has a local maximum with respect to time τ, when ψ exhibits a corresponding minimum in time, which is the case for $\alpha \in (0,1)$. For all other α the E monotonically decreases with time from its initial value $E(\psi_0)$.

Inserting the solution (55) provides for Eq. (36), $d\psi/d\tau = \alpha - \Phi$, the nonlinear differential equation

$$\frac{d\psi}{d\tau} = \alpha\left[1 + W\left(-\frac{E(\psi)}{\alpha}\right)\right], \tag{57}$$

with the function E from (56). Making use of the initial condition (33) this readily integrates to

$$\tau = \frac{1}{\alpha}\int_{\psi_0}^{\psi} \frac{dx}{1 + W\left(-\frac{E(x)}{\alpha}\right)} \tag{58}$$

We thus arrived at an exact analytical solution of the SIRV equations. We call this an inverse solution, as we have expressed τ in terms of ψ and not vice versa. This is a remarkably compact result, especially, as we know already that $\psi(\tau)$, for the relevant case of $\alpha \in [0,1]$, is not a monotonous function, while we should come up with a unique ψ for each τ.

The solution to this at first sight apparent contradiction is provided by the two real-valued Lambert functions $W_0(x)$ and $W_{-1}(x)$, that have different values over a range of negative $x \in [-e^{-1}, 0]$ values. For positive arguments x, only $W_0(x)$ is real-valued. The range of application of the two Lambert functions will be discussed in Appendix A. Here we state the main outcome of these considerations.

As long as ψ exhibits a minimum, which is the case for all $\alpha \in (0,1)$, Eq. (58) must be interpreted as

$$\tau = \begin{cases} \frac{1}{\alpha}\int_{\psi_0}^{\psi} \frac{dx}{1+W_{-1}\left(-\frac{E(x)}{\alpha}\right)}, & \psi \le \psi_m, \\ \tau_m + \frac{1}{\alpha}\int_{\psi_m}^{\psi} \frac{dx}{1+W_0\left(-\frac{E(x)}{\alpha}\right)}, & \psi \ge \psi_m \end{cases} \tag{59}$$

or alternatively, in a more symmetric fashion, as

$$\tau = \tau_m + \begin{cases} \frac{1}{\alpha}\int_{\psi_m}^{\psi} \frac{dx}{1+W_{-1}(z(x))}, & \psi \le \psi_m \\ \frac{1}{\alpha}\int_{\psi_m}^{\psi} \frac{dx}{1+W_0(z(x))}, & \psi \ge \psi_m \end{cases} \tag{60}$$

where the crossover is located at $\Phi = \alpha$, i.e., where $\psi = \psi_m$ has reached its minimum, and the time where this minimum occurs, is given by

$$\tau_m = \frac{1}{\alpha}\int_{\psi_0}^{\psi_m} \frac{dx}{1 + W_{-1}\left(-\frac{E(x)}{\alpha}\right)} \tag{61}$$

In the absence of a minimum of ψ, i.e., for $\alpha \notin (0,1)$, there is no crossover, the ψ is monotonous, and one can use Eq. (58) throughout. For $\alpha < 0$ the argument of the Lambert function is positive, so that one has to use Eq. (58) with $W = W_0$.

For $\alpha > 1$, the minimum of ψ coincides with ψ_0, hence $\tau_m = 0$, so that only the 2nd term in the 2nd case of Eq. (60) survives, again involving the principal W_0 only. The non-principal Lambert function W_{-1} thus only plays a role in the case $\alpha = k - b \in (0,1)$.

3.5. Determination of the minimum value ψ_m for $\alpha \in (0,1)$

To evaluate τ given by Eq. (60) for the case of $\alpha \in (0,1)$ we need to specify ψ_m. We have noted before (see Eq. (36)) that the function ψ attains its minimum value ψ_m at $\Phi_m = \alpha$, and that a minimum exists for all $\alpha \in (0,1)$. According to the solution (55) we

Preprints (www.preprints.org) | NOT PEER-REVIEWED | Posted: 30 March 2021 doi:10.20944/preprints202103.0718.v1

find the minimum value ψ_m from $\Phi_m = \alpha = -\alpha W(-E_m/\alpha)$, where $E_m = E(\psi_m)$, yielding $W(-E_m/\alpha) = -1$. Both, the principal and non-principal, Lambert functions have the same value -1 at the argument $(-e^{-1})$ so that $E_m = \alpha/e$. This yields with Eq. (54) the equation that determines ψ_m,

$$\frac{e^{\frac{k}{\alpha}(\psi_m-\psi_0)}}{1+e^{\psi_m}} = \frac{\eta}{\alpha}e^{1-(1/\alpha)} \tag{62}$$

Because ψ_m is the value at the minimum, $\psi_m \leq \psi_0$ automatically holds. This nonlinear equation for ψ_m cannot be solved analytically in general. For some special cases such as $b = k/2$ one can still write down an analytical solution. An approximant for ψ_m will be derived below.

4. Approximated reduction of the exact solution

4.1. Approximate inverse solution $\tau(\psi)$

Here we derive an approximant for the exact inverse solution $\tau(\psi)$, that can be later inverted exactly to obtain $\psi(\tau)$ in the next subsection. Upon introducing $z = -E(x)/\alpha$ with $E(x)$ given by Eq. (56) the previous inverse solutions (58) and (60) for τ, and also τ_m defined by Eq. (61), are of the form

$$\begin{aligned} \tau &= \frac{1}{\alpha}\int_{\psi_1}^{\psi_2} \frac{dx}{1+W_\mu(-\frac{E(x)}{\alpha})} \\ &= \frac{1}{\alpha}\int_{z(\psi_1)}^{z(\psi_2)} \frac{dz}{(dz/dx)[1+W_\mu(z)]} \end{aligned} \tag{63}$$

where ψ_1, ψ_2 and $\mu = 0$, or $\mu = -1$ are treated as arbitrary coefficients for the time being, as W_μ stands for any of the two Lambert functions, so that τ is of the form (63) for any $\alpha \notin \{0,1\}$. Evaluating the required derivative of z with respect to x gives

$$\frac{dz}{dx} = \left(\frac{1}{1+e^{-x}} - \frac{k}{\alpha}\right)z \tag{64}$$

The 1st term can be approximated by unity when $x \gg 1$ and thus $e^{-x} \ll 1$, and k/α not too close to unity, i.e., b not too small. The precise range of validity of this approximation will be worked out in Appendix B and section 4.4, where we specify a critical b_c below which the current approximation need not be used. For $\alpha > 1$ and $\alpha < 0$ one has $e^{-x} < e^{-\psi_0}$ so that this approximation is applicable for any $\eta \ll 1$ when $\alpha \notin [0,1]$. For $\alpha \in (0,1)$ one has $e^{-x} < e^{-\tau_m}$ so that the approximation is excellent as long as $\tau_m \gg 1$. Under such circumstances, i.e., for $b > b_c$, Eq. (64) is well approximated as

$$\frac{dz}{dx} \simeq \left(1 - \frac{k}{\alpha}\right)z = -\frac{b}{\alpha}z \tag{65}$$

with $\alpha = k - b$. Hence Eq. (63) is well approximated by

$$\tau \simeq \frac{1}{b}\int_{z(\psi_2)}^{z(\psi_1)} \frac{dz}{z[1+W_\mu(z)]} \tag{66}$$

Then with the substitution $z = we^w$, corresponding to $w = W_\mu(z)$, and $dz/dw = (1+w)e^w$ we can calculate the integral (66) in closed form as

$$\tau = \frac{1}{b}\int_{W_\mu(z(\psi_2))}^{W_\mu(z(\psi_1))} \frac{dw(1+w)e^w}{we^w(1+w)} = \frac{1}{b}\int_{W_\mu(z(\psi_2))}^{W_\mu(z(\psi_1))} \frac{dw}{w} = \frac{1}{b}\ln\left[\frac{-W_\mu(z(\psi_1))}{-W_\mu(z(\psi_2))}\right] \tag{67}$$

The minus sign is kept in nominator and denominator as the W_μ is typically negative. For $\alpha \in (0,1)$ the ψ initially decays with time, until it reaches its minimum ψ_m. At the minimum $W_\mu(z(\psi_m)) = -1$. Because $W_\mu(z) = 0$ only for $z = 0$, and because $E(x)$ is

Preprints (www.preprints.org) | NOT PEER-REVIEWED | Posted: 30 March 2021 doi:10.20944/preprints202103.0718.v1

positive for all $\eta > 0$, Eq. (67) has removed the problem with the pole that occurs at $z = e^{-1}$ in the starting Eq. (63).

Having arrived at Eq. (67) we can now identify placeholders ψ_1, ψ_2 and μ in the three equations (58) with $\mu = 0$, (60), and (61) to write down τ for the various cases, as well as τ_m. We begin with the case of $\alpha \in (0,1)$ and $\psi \leq \psi_m$. Upon comparing the first line in Eq. (60) with Eq. (63), we need to use $\psi_1 = \psi_m$ and $\psi_2 = \psi$ and $\mu = -1$ for the regime $\psi \leq \psi_m$. Because α is positive, and z thus negative, using Eq. (67), this becomes immediately

$$\tau = \tau_m + \frac{1}{b} \ln\left[\frac{-W_{-1}(z(\psi_m))}{-W_{-1}(z(\psi))}\right], \quad (\alpha \in (0,1), \psi \leq \psi_m) \tag{68}$$

Because $z(\psi_m) = -1/e$, $W_\mu(-1/e) = -1$, the term $\ln[-W_\mu(-1/e)] = \ln(1) = 0$ vanishes for both μ. The nominator in Eq. (68) can thus be replaced by unity. Exactly the same procedure, applied to the remaining cases yields our final expression for the approximate inverse solution when $\alpha \in (0,1)$,

$$\tau \quad = \quad \begin{cases} \tau_m - \frac{1}{b} \ln[-W_{-1}(-E(\psi)/\alpha)], & 0 \leq \tau \leq \tau_m, \\ \\ \tau_m - \frac{1}{b} \ln[-W_0(-E(\psi)/\alpha)], & \tau \geq \tau_m \end{cases} \tag{69}$$

with $E(\psi)$ given by Eq. (56). Similarly, the time τ_m can be read off from Eq. (67) by choosing $\psi_1 = \psi_0$, $\psi_2 = \psi_m$, and $\mu = -1$. Hence

$$\tau_m = \frac{1}{b} \ln\left[-W_{-1}\left(-\frac{e^{-1/\alpha}}{\alpha}\right)\right] = -\frac{\ln(\alpha)}{b} \tag{70}$$

where we have used $E(\psi_0) = e^{-1/\alpha}$ and $E(\psi_m)/\alpha = 1/e$ and the identity $-\alpha W_{-1}(z(\psi_0)) = 1$ (proof in Appendix C) to simplify the expression. Such time τ_m only exists for $\alpha \in (0,1)$.

There is the remaining case of $\alpha \notin [0,1]$. Equation (58) implies using $\psi_1 = \psi_0$, $\psi_2 = \psi$, and the principal Lambert function ($\mu = 0$), as discussed already. Because $z(\psi)$ and thus $W_0(z(\psi))$ have different signs for $\alpha < 0$ and $\alpha > 1$, we multiply both the nominator and denominator in Eq. (67) by α to get rid of two different signs for positive and negative α. At the same time, because of the identity $-\alpha W_0(z(\psi_0)) = 1$ (proof in Appendix C) that holds for all $\alpha \notin (0,1)$, the logarithm of this quantity vanishes, and we arrive at the final expression for the approximate inverse solution valid for all $\tau \geq 0$ and all $\alpha \notin [0,1]$,

$$\tau = -\frac{1}{b} \ln[-\alpha W_0(-E(\psi)/\alpha)] \tag{71}$$

Notice that the argument of the logarithm is positive for both $\alpha < 0$ and $\alpha > 1$.

It is important to realize that the value for ψ_m has completely disappeared within the approximate case. Still, we can use a very similar approximation done here to obtain an explicit expression for ψ_m, that might be helpful for the evaluation of the exact inverse solution and the exact ψ_m as long as $\alpha \in (0,1)$. If b is not too small, we can approximate the $1 + e^{\psi_m}$ in the Eq. (62) determining ψ_m by e^{ψ_m} and solve for ψ_m analytically. This yields (Fig. 2)

$$\psi_m \simeq \psi_0 - \frac{1 - \alpha + \alpha \ln \alpha - \alpha \ln(1-\eta)}{b} \tag{72}$$

Note that this value has the feature $W_{-1}[-E(\psi_m)/\alpha] = -1$ for $\eta = 0$. In practise, for $\eta \ll 1$, the $\ln(1-\eta)$ term can be safely neglected and we shall use

$$\psi_m \simeq \psi_0 - \frac{1 - \alpha + \alpha \ln \alpha}{b} \tag{73}$$

while it possible to add this $\ln(1-\eta)$ correction throughout the rest of this document.

Preprints (www.preprints.org) | NOT PEER-REVIEWED | Posted: 30 March 2021 doi:10.20944/preprints202103.0718.v1

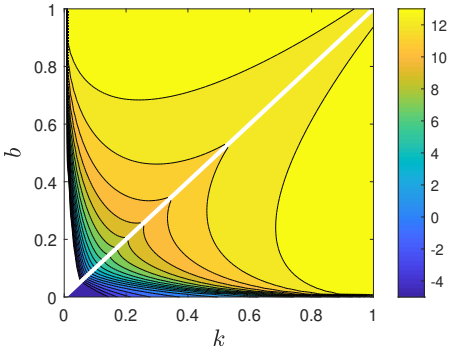

Figure 2. Exact ψ_m versus k and b in the lower right triangle, and approximate ψ_m using Eq. (73) above the diagonal (mirrored, to allow for a simple comparison with the exact ψ_m). All analytic results for the SIRV functions in terms of reduced time τ are basically exact for those k and b for which ψ_m is well described by its approximant. The white space in the lower left corner is the regime of $b < b_c$, where the SIRV model results are captured by linearly interpolating between the SIR model and the SIRV model evaluated at the critical $b = b_c$.

4.2. Approximate direct solution $\psi(\tau)$

Next we invert the approximate inverse solution to come up with an approximate direct solution of the SIRV equations. With Eqs. (69)–(71) we have provided approximate expressions for τ_m, and τ as function of ψ, for any negative or positive α. Fortunately, we can proceed and invert the relationships without any further assumption to come up with the corresponding, much more convenient, explicit solution $\psi(\tau)$. Because we have expressed all SIRV functions in terms of ψ, we then have access to all these quantities in terms of reduced time τ.

We begin with an illustrative example. In Eq. (70) we have provided τ_m in terms of b and α. We can invert the relationship to obtain α from τ_m and b as follows

$$\frac{e^{-1/\alpha}}{\alpha} = \exp\left(b\tau_m - e^{b\tau_m}\right) \tag{74}$$

To prove the equivalence between Eq. (74) and Eq. (70), one has to just insert Eq. (74) into Eq. (70) and to use the fact that the Lambert function $W(x)$ is the inverse function of $x(W) = We^W$. More specifically, consider $y(\zeta) = \ln[-W(\zeta)]$. Its inverse is given by $\zeta(y) = -\exp[y - e^y]$ because $\zeta(y) = -\exp[\ln(-W(\zeta)) - e^{\ln(-W(\zeta))}] = W(\zeta)e^{W(\zeta)} = \zeta$. To derive Eq. (74) we had thus identified $\zeta = -e^{-1/\alpha}/\alpha$ and $y(\zeta) = b\tau_m$. The same procedure can be applied to all expressions from the previous section using different choices for y and ζ.

One more required ingredient is however an expression for ψ in terms of E. It can be readily deduced using the existing assumption that lead to Eq. (73). To derive this Eq. (73) we assumed that $1 + e^{\psi_m} \approx e^{\psi_m}$. Since the minimum $\psi_m \leq \psi$ at all times, the assumption $1 + e^{\psi} \approx e^{\psi}$ is even more appropriate within all remaining times. With this replacement Eq. (56) becomes

$$E(\psi) \simeq \eta \exp\left[\frac{k\psi_0 - 1 - b\psi}{\alpha}\right] \tag{75}$$

and this can be solved for ψ to arrive at

$$\begin{aligned} \psi(\tau) &\simeq \psi_0 - \frac{1 - \alpha\ln(1-\eta) + \alpha\ln[\mathcal{E}(\tau)]}{b} \\ &= \psi_m - \frac{\alpha}{b}\ln\frac{e\mathcal{E}(\tau)}{\alpha} \end{aligned} \tag{76}$$

with $\mathcal{E}(\tau) = E(\psi(\tau))$ and where we used Eq. (72). We here introduced the symbol $\mathcal{E}$ instead of E only to highlight the different argument and to avoid potential confusion.

Preprints (www.preprints.org) | NOT PEER-REVIEWED | Posted: 30 March 2021 doi:10.20944/preprints202103.0718.v1

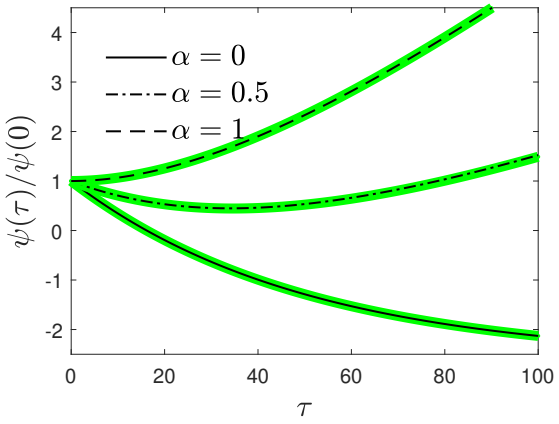

Figure 3. Comparison of the approximant Eq. (79) for $\psi(\tau)/\psi_0$ with the exact solution (black lines) Eqs. (58) and (60) for three different α's at $\eta = 10^{-6}$ a relatively low $b = 0.02$. For the approximant (green), the ψ_m and τ_m are given by Eqs. (73) and (70), respectively. For larger b the performance of the approximant is even better.

Note that this generalization of Eq. (73) is compatible with the special case $\psi_m = \psi(\tau_m)$ because $\mathcal{E}(\tau_m) = E(\psi_m) = \alpha/e$. As before it is even more convenient to drop a term of $O(\eta)$ so that $\psi(0)$ coincides with the exact value. Since $\mathcal{E}(0) = E(\psi_0) = e^{-1/\alpha}$, the correction results in the simpler

$$\psi(\tau) = \psi_0 - \frac{1 + \alpha \ln[\mathcal{E}(\tau)]}{b} \tag{77}$$

Having expressed ψ in terms of τ and $\ln[\mathcal{E}(\tau)]$, we are left to write down expressions for $\ln[\mathcal{E}(\tau)]$. With such expressions at hand, Eq. (77) is our explicit solution of the SIRV equations. The $\ln[\mathcal{E}(\tau)]$ depends on the α range.

For $\alpha \in (0, 1)$, in view of Eq. (69), we need to use $y(\zeta) = b(\tau_m - \tau)$ and $\zeta = z(\psi) = -E(\psi)/\alpha$ to obtain the explicit $\zeta(y) = -\exp[y - e^y]$, or equivalently, $\ln[-\zeta(y)] = y - e^y$. Replacing y and ζ, we thus find for $\alpha \in (0, 1)$

$$\ln[\mathcal{E}(\tau)] = \ln(\alpha) - b(\tau - \tau_m) - e^{-b(\tau - \tau_m)} \tag{78}$$

Note that there is no need to consider two regimes before and after the peak anymore! While the two Lambert functions W_0 and W_1 are very different, they share a common inverse, and Eq. (78) is valid over the whole $\tau \geq 0$ range.

To summarize, upon inserting Eq. (78) into Eq. (77), we end up with a final expression for $\psi(\tau)$ for all $\alpha \in (0, 1)$,

$$\begin{aligned} \psi(\tau) &= \psi_m + \alpha(\tau - \tau_m) - \frac{\alpha}{b}\left[1 - e^{-b(\tau - \tau_m)}\right] \\ &= \psi_0 + \alpha\tau - \frac{1 - e^{-b\tau}}{b} \end{aligned} \tag{79}$$

where we have used τ_m and ψ_m from Eqs. (70) and (73) to arrive at the 2nd line. In Fig. 3 we compare the approximant Eq. (79) with the exact solution for two different α's. For the remaining cases of $\alpha \notin [0, 1]$ we have to invert Eq. (71). Repeating the above procedure, one has $\ln[\mathcal{E}(\tau)] = -b\tau - \alpha^{-1}\exp(-b\tau)$ for $\alpha \notin [0, 1]$. Upon inserting this term into Eq. (77), one arrives at the explicit approximate solution of the SIRV equations for $\alpha \notin (0, 1)$

$$\psi(\tau) = \psi_0 + \alpha\tau - \frac{1 - e^{-b\tau}}{b} \tag{80}$$

Not only is this result exactly of the form we obtained for $\alpha \in (0, 1)$, it is moreover valid also for the special values of $\alpha = 0$ and $\alpha = 1$, as all – at first glance problematic – divergencies

Preprints (www.preprints.org) | NOT PEER-REVIEWED | Posted: 30 March 2021 doi:10.20944/preprints202103.0718.v1

have dropped out. From Eq. (80) we can see that $\psi_\infty = \lim_{\tau\to\infty}\psi(\tau) = \text{sign}(\alpha)\infty$ except for $\alpha = 0$ or $b = k$, where $\psi_\infty = \psi_0 - 1/k$ approaches a finite value. The full expression valid for all α is thus

$$\psi_\infty = \left(\psi_0 - \frac{1}{k}\right)\delta_{\alpha,0} + (1-\delta_{\alpha,0})\text{sign}(\alpha)\infty \tag{81}$$

in full accord with the exact SIRV solution.

4.3. Time-dependency of all remaining SIRV quantities

With $\psi(\tau)$ given by Eq. (80) and the corresponding

$$\Phi(\tau) = \alpha - \frac{d\psi}{d\tau} = e^{-b\tau} \tag{82}$$

for all values of α at hand it is now straightforward to write down all remaining SIRV quantities, as we have expressed them in terms of ψ above. It is perhaps interesting to note that the approximant shares the most relevant features with the exact solution: $\psi(\tau_m) = \psi_m$, $\psi(0) = \psi_0$, $\Phi(0) = 1$, and $\psi'(0) = \alpha - 1$ (as required by Eq. (37)) for all α. In the limit of infinitely long times, $\Phi_\infty = 0$, according to Eq. (82) unless $b = 0$.

All remaining SIRV quantities are obtained using $\psi(\tau)$ and $\Phi(\tau)$ from Eqs. (80) and (82) via

$$\begin{aligned}
S(\tau) &= \frac{\Phi(\tau)}{1+e^{-\psi(\tau)}} && (83)\\
I(\tau) &= \frac{\Phi(\tau)}{1+e^{\psi(\tau)}} && (84)\\
j(\tau) &= S(\tau)I(\tau), && (85)\\
J(\tau) &= \eta + \int_0^\tau j(\tau')d\tau', && (86)\\
R(\tau) &= J(\tau) - I(\tau), && (87)\\
V(\tau) &= 1 - S(\tau) - J(\tau) && (88)
\end{aligned}$$

For $\alpha = 0$, where we can use $\psi(\tau)$ from Eq. (80) with $b = k$, these expressions solve the SIRV equations (12)–(14) exactly, as can be verified by direct insertion into Eqs. (12)–(15). An alternative proof is provided in Appendix G.1. Otherwise they solve the SIRV equations to within $O(\eta)$. The version $J(\tau)$ given by Eq. (86) ensures that $j = dJ/d\tau$ holds exactly.

It is a rather tedious exercise to insert the ψ and Φ into Eqs. (84)–(88). In evaluating the limiting values for $\tau \to \infty$ one has to carefully consider the qualitatively different regimes $\alpha < 0$, $\alpha = 0$, $\alpha \in (0,1)$ and $\alpha \geq 1$, as well as $k = 0$ when $\alpha = 0$. This can be done but we refrain from writing down all equations for the approximate explicit solution of the SIRV equations. Instead, we provide in Appendix G exact solutions for special cases, and compare the approximate explicit solution with the exact numerical solution for several cases. To provide an example, inserting ψ (80) and Φ (82) into the expressions for S (83) and I (84) yields

$$\begin{aligned}
S(\tau) &= \frac{e^{-b\tau}}{2}\left\{1 + \tanh\left[\frac{\alpha b\tau + b\psi_0 + e^{-b\tau} - 1}{2b}\right]\right\}, && (89)\\
I(\tau) &= \frac{e^{-b\tau}}{2}\left\{1 - \tanh\left[\frac{\alpha b\tau + b\psi_0 + e^{-b\tau} - 1}{2b}\right]\right\} && (90)
\end{aligned}$$

Next, we focus on the most relevant. measurable features of the SIRV model, that derive from the analytic approximant.

Preprints (www.preprints.org) | NOT PEER-REVIEWED | Posted: 30 March 2021 doi:10.20944/preprints202103.0718.v1

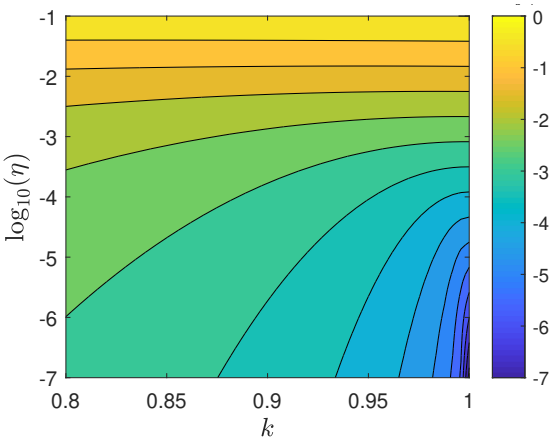

Figure 4. The critical b_c versus k and η. The coloring scheme uses the decadic logarithm of b_c, and the vertical axis is also logarithmic. Shown is only a relevant range of k values.

4.4. Critical reduced vaccination rate b

As we will demonstrate below, the approximants (80) and (82) capture the exact solution very well (or also exactly for some special cases like $\alpha = 0$) except for the regime where b stays below a critical b_c. The limiting case of $b = 0$ is known as SIR model and had been treated elsewhere so that the failure of our approximant does not seem to pose a problem. It is however possible to quantify the range of validity of Eqs. (80) and (82). This is done in Appendix B and leads to a critical value b_c in terms of η and k

$$b_c = \left(32\pi k\eta^2\right)^{3/5} \exp\left\{W_0\left[\frac{6(1-k+k\ln k)}{5(32\pi k\eta^2)^{3/5}}\right]\right\} \tag{91}$$

for the reduced vaccination rate, beyond which the approximant is very accurate. See Fig. 4 for a plot of b_c versus k and η. The critical b_c decreases with increasing k and decreasing η, while it is quite sensitive to k for values close to unity. At $k = 1$, Eq. (91) evaluates to $(32\pi\eta^2)^{3/5} \approx 15.9 \times \eta^{6/5}$ and b_c is thus roughly proportional to η in that case.

For the remaining range of b values below b_c we can make use of the known solution of the SIR model, that corresponds to the SIRV model with $b = 0$. To be specific, the characteristics of time-evolution such as peak time and height of the differential rate, or the final fraction of infected population are well captured by a simple linear interpolation between SIRV values at $b = b_c$ and the SIR values. This will be worked out next to conclude with approximants that are valid for any b.

4.5. Peak times and peak amplitudes

While $S(\tau)$ decreases monotonically with time, both $I(\tau)$ and $j(\tau) = S(\tau)I(\tau)$ exhibit a maximum, whose position and amplitude we can calculate from Eqs. (89) and (90). While the general case of arbitrary η is treated in Appendices E amd F, we here limit the analysis to the relevant case of a small initially (and simultaneously) infected fraction $\eta \ll 1$ of the population. In this limit we obtain to leading order for all α

$$I(\tau) \simeq \eta e^{\frac{1-e^{-b\tau}}{b} - k\tau} + \mathcal{O}(\eta^2), \tag{92}$$
$$S(\tau) \simeq e^{-b\tau} + \mathcal{O}(\eta), \tag{93}$$

implying for the differential fraction of newly infected persons

$$j(\tau) \simeq \eta e^{\frac{1-e^{-b\tau}}{b} - (k+b)\tau} + O(\eta^2) \tag{94}$$

Preprints (www.preprints.org) | NOT PEER-REVIEWED | Posted: 30 March 2021 doi:10.20944/preprints202103.0718.v1

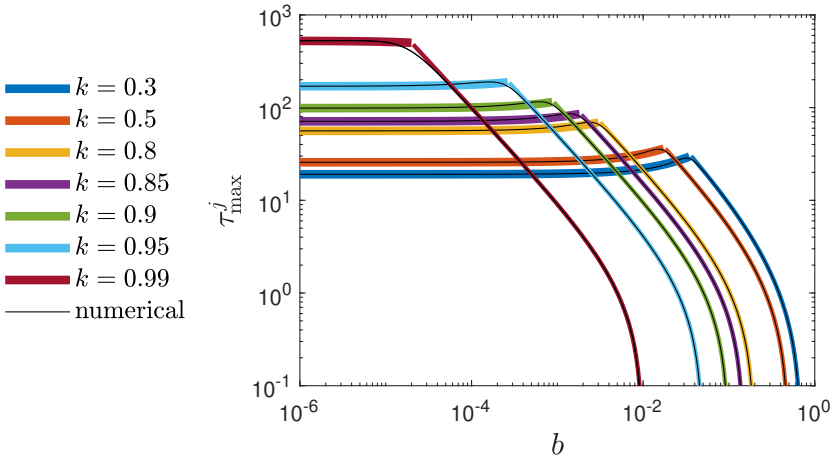

Figure 5. Reduced peak time $\tau^j_{\max}$ of the newly infected population fraction $j(\tau)$ versus b for various k at $\eta = 10^{-6}$ (double-logarithmic). The exact numerical solution (solid black) is compared with the approximant (97) within the regime of $b > b_c$ (thin colored), and by the corresponding linear interpolant (thick colored) for the remaining regime of very small $b < b_c$. The limiting value $\tau^j_{\max}(b \to 0)$ exactly coincides with the $\tau^{\mathrm{SIR}}_{\max}(k)$ of the SIR model (Appendix G.2).

The peak time of the maximum in $I(\tau)$ is thus

$$\tau^I_{\max} = -\frac{\ln(k)}{b} + O(\eta), \tag{95}$$

so that a peak in I thus exists only if $k < 1$. For the fraction of currently infected persons at peak time we have

$$I_{\max} = I(\tau^I_{\max}) \simeq \eta e^{1/b} \left(\frac{k}{e}\right)^{k/b} + O(\eta^2) \tag{96}$$

Likewise, the peak time of the maximum in $j(\tau)$ is at (thin colored lines in Fig. 5)

$$\tau^j_{\max} = -\frac{\ln(k+b)}{b} + O(\eta), \tag{97}$$

where j achieves the value

$$j_{\max}(k,b) = \eta e^{1/b} \left(\frac{k+b}{e}\right)^{(k+b)/b} \tag{98}$$

or equivalently, as the following expression is much more conveniently evaluated at small b (thin colored lines in Fig. 6)

$$\ln j_{\max}(k,b) = \ln(\eta) - 1 + \frac{1-k}{b} + \frac{k+b}{b}\ln(k+b) \tag{99}$$

A peak in j thus occurs only for $k + b < 1$, in agreement with our earlier consideration (see Eq. (10)), as we assume small $\eta \ll 1$ here. While the peak time $\tau^j_{\max}$ increases with increasing b in the regime of $b < b_c$, it decays with b for $b > b_c$.

The maximum rate (98) is not applicable for $b < b_c$ below a critical, very small b_c, given by Eq. (91). For small $b < b_c$ we can make use of the known [3] exact result $j^{\mathrm{SIR}}_{\max}$ of the SIR model, reproduced in Eq. (A62), and linearly interpolate as (thick colored lines in Fig. 6)

$$j_{\max}(k,b) = \frac{b}{b_c} j_{\max}(k,b_c) + \frac{b_c - b}{b_c} j^{\mathrm{SIR}}_{\max}(k) \tag{100}$$

Preprints (www.preprints.org) | NOT PEER-REVIEWED | Posted: 30 March 2021 doi:10.20944/preprints202103.0718.v1

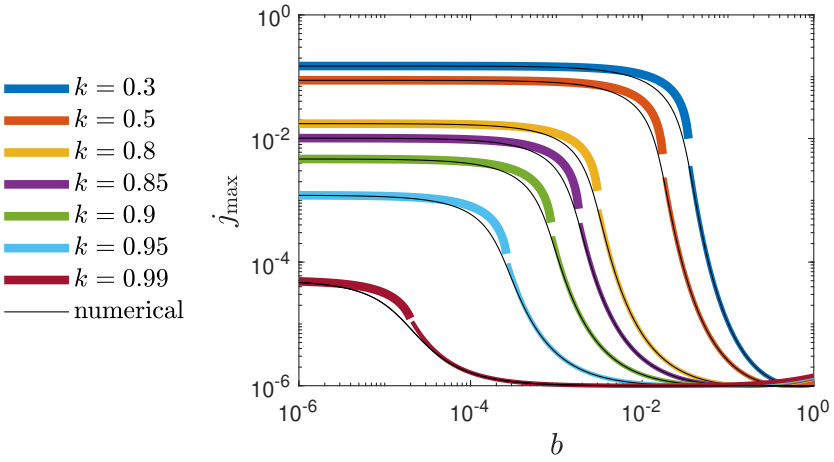

Figure 6. Peak value of the newly infected population fraction $j_{\max}$ versus reduced vaccination rate b for various k at $\eta = 10^{-6}$ (double-logarithmic). The exact numerical solution (solid black) is compared with the approximant (98) within the regime of $b > b_c$ (thin colored), and by the interpolant (100) (thick colored) for the remaining regime of very small $b < b_c$. The limiting value $j_{\max}(b \to 0)$ exactly coincides with the $j_{\max}^{\mathrm{SIR}}(k)$ of the SIR model (Appendix G.2).

where $j_{\max}(k, b_c)$ and $j_{\max}^{\mathrm{SIR}}(k)$ are given by Eqs. (98) (evaluated at $b = b_c$) and (A62), respectively. The analytical expressions for time and amplitude of the daily number of infected persons are two of the more important results of this study. They can be immediately used to rate the effect of vaccination rate for all b, using Eq. (98) for $b \geq b_c$ and Eq. (100) for $b < b_c$, where the critical rate b_c is given by Eq. (91).

One should keep in mind that the maximum of the $j(\tau)$ is not located at $\tau = \tau_m$, which marks the time of the minimum in $\psi(\tau)$. And there is also a remaining apparent contradiction. While the initial slope of $j(\tau)$ is positive for $k + b < 1 - 2\eta$ and $j(\tau)$ thus going through a peak at a future time in that case, and taking identical values at different times, the $\psi(\tau)$ exhibits a minimum for all $\alpha \in (0, 1)$. Under such latter conditions, there are at least two times that exhibit the same ψ value. The apparent contradiction finds its explanation in the fact that $j(\tau)$ cannot be expressed in terms of $\psi(\tau)$ alone, but also involves the derivative of ψ with respect to τ, which is contained in Φ. In other words, both Lambert functions are sometimes (when $k - b \in (0, 1)$ and $k + b > 1 - 2\eta$) required to describe a $j(\tau)$ that is monotonically decreasing, and a single Lambert function is sometimes (when $k - b \notin [0, 1]$ and $k + b < 1 - 2\eta$) sufficient to describe a $j(\tau)$ that exhibits a maximum. Another way to understand this feature is the fact, that the expressions for the SIRV quantities have the same form irrespective the value for α, i.e., irrespective the occurrence of a minimum in $\psi(\tau)$.

4.6. Total fraction of infected persons

The differential $j(\tau)$ given by Eq. (94) can be integrated to obtain the cumulative fraction $J(\tau)$ as shown in Appendix D. For J_∞ we thus obtain (thin colored lines in Fig. 7)

$$J_\infty(k, b) = \eta k b^{\frac{b}{k}-1} e^{\frac{1}{b}} \gamma\left(\frac{k}{b}, \frac{1}{b}\right) \tag{101}$$

in terms of the lower incomplete gamma function γ [12]. For the special case of $\alpha = 0$ ($k = b$), the Eq. (101) agrees with the exact result (A53) up to order $O(\eta^2)$. As for $j_{\max}$, we have to distinguish two regimes: (i) the regime of $b > b_c$, where this expression (101) is useful, (ii) the regime of small $b < b_c$, for which we need, on one hand, the known exact result of the SIR model, J_∞^{SIR}, and on the other, the value for J_∞ given by Eq. (101), evaluated at $b = b_c$. Since b_c is so very small, the direct insertion into (101) is numerically impossible. We therefore derive in Eq. (A15) of Appendix D a limiting expression valid for small values

Preprints (www.preprints.org) | NOT PEER-REVIEWED | Posted: 30 March 2021 doi:10.20944/preprints202103.0718.v1

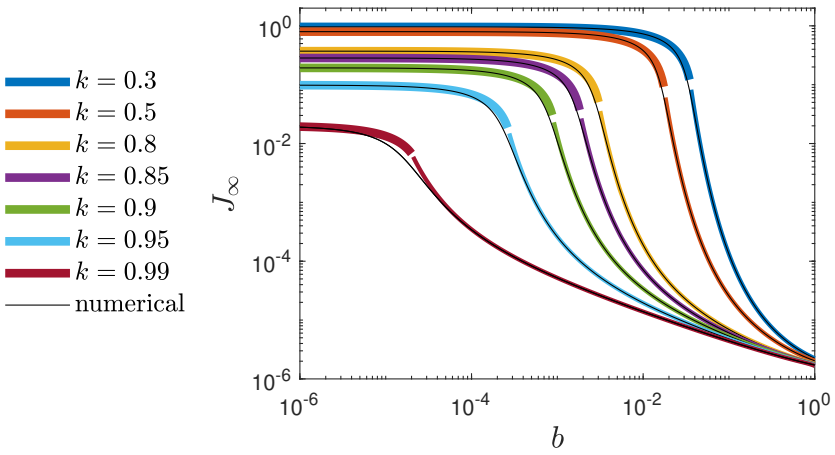

Figure 7. Final fraction of infected persons J_∞ versus reduced vaccination rate b for various k at $\eta = 10^{-6}$ (double-logarithmic). The exact numerical solution (solid black) is compared with the approximant (101) within the regime of $b > b_c$ (thin colored), and by the interpolant (102) (thick colored) for the remaining regime of very small $b < b_c$. The limiting value $J_\infty(b \to 0)$ exactly coincides with the $J_\infty^{\mathrm{SIR}}(k)$ of the SIR model (Appendix G.2).

of b such as $b = b_c$, that enters the following Eq. (102). Using exactly the same interpolation approach as before for $j_{\max}$, the J_∞ within the regime of small $b < b_c$ is approximated with the help of Eq. (101) by (thick colored lines in Fig. 7)

$$J_\infty(k,b) = \frac{b\eta}{b_c}\sqrt{\frac{2\pi k}{b_c}}e^{\frac{1-k+k\ln k}{b_c}} + \frac{b_c - b}{b_c}J_\infty^{\mathrm{SIR}}(k) \tag{102}$$

where $J_\infty^{\mathrm{SIR}}(k)$ is the known analytical expression for the SIR model, reproduced in Eq. (A61), and b_c is given by Eq. (91).

4.7. Differential rate

We next provide an analytical approximant for the time-dependent differential rate $j(\tau)$, valid for any b, and small $\eta \ll 1$. For b exceeding the critical b_c, we can just use the expression (94). The comparison with the analytic result is excellent (Fig. 8a–c). For $b < b_c$, on the other hand, we have shown already that the peak time and peak amplitude are well approximated analytically by a linear superposition between the SIRV approximant evaluated at the critical b_c, and the analytical SIR expression. The analytical expression for the full time-dependency of $j(\tau)$ in this subcritical regime of $b < b_c$ is therefore not just a linear superposition of the $j(\tau)$ for SIRV and SIR model, because such superposition would not recover the already determined peak time and height. Instead, as we demonstrate with Fig. 8(d–f), and inspired by the earlier observation that the Gauss model [13,14] captures the differential rate very well, the $j(\tau)$ is well described for $b < b_c$ by the Gaussian

$$j(\tau) = j_{\max}\exp\left[-\frac{(\tau - \tau_{\max}^j)^2}{w^2}\right] \tag{103}$$

with a width w that is determined by [13]

$$w = \frac{J_\infty}{\sqrt{\pi}j_{\max}} \tag{104}$$

where $j_{\max}$ and J_∞ are given by Eqs. (100) and (102), respectively.

Preprints (www.preprints.org) | NOT PEER-REVIEWED | Posted: 30 March 2021 doi:10.20944/preprints202103.0718.v1

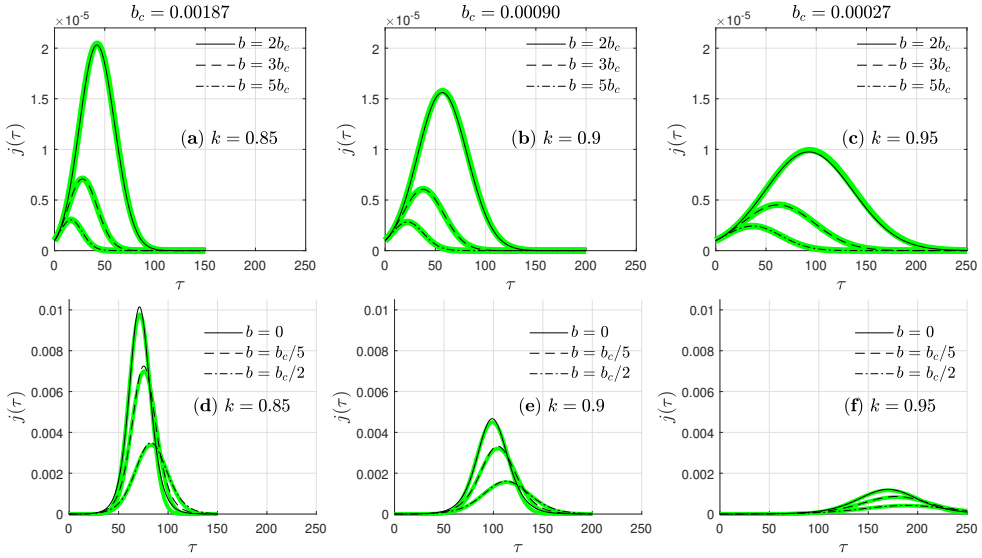

Figure 8. Differential rate $j(\tau)$ of infected population fraction versus reduced time τ for three different $k \in \{0.85, 0.90, 0.95\}$ and various reduced vaccination rates b/b_c. For this plot $\eta = 10^{-6}$. The panels (**a**)–(**c**) show the regime $b > b_c$, while (**d**)–(**f**) show results for $b < b_c$ including $b = 0$ (SIR model). To rate the effect of the parameters, all three plots of each row are shown on identical scales. While the peak time increases with increasing k and decreasing b, the peak height dramatically decreases with increasing b. The critical b_c depends on k and η, c.f., Eq. (91) and Fig. 4. The area under the curves is the total cumulative fraction J_∞ of infected persons. The black lines are exact numerical results, the green lines are our analytical approximant, provided in Section 4.7.

4.8. Time scales

Summarizing our analysis here we emphasize that SIRV-pandemic waves in the case $0 < b \ll \alpha < 1$ exhibit a clear asymmetry with respect to peak time in reduced and real time. The fraction of infected (I) and recovered (R) persons as well as the daily rate of new infections (j) vary rapidly on the order of the recovery reduced time scale $\tau_r \simeq \alpha^{-1} \simeq k^{-1}$, corresponding to recovery real time scale $T_r \simeq 1/\mu(0)$. Alternatively, the fraction of susceptible (S) and vaccinated (V) persons as well as the sum $\Phi = S + I$ vary slowly on the order of the much greater vaccination reduced time scale $\tau_v \simeq b^{-1}$, corresponding to the vaccination real time scale $T_v \simeq 1/v(0)$. Thirdly, the cumulative fraction of newly infected persons $J(\tau)$ exhibits an asymmetric time structure determined both by τ_r and τ_v. These behaviors are clearly visible in Fig. 9(b-d) or alternatively Fig. 9(f-h), where we show the time distribution of all SIRV quantities in one plot for different values of b at $k = 0.9$. The behavior is qualitatively similar but quantitatively different for other values of k. Comparing the asymmetric time distribution of $J(\tau)$ with empirical data then should allow the determination of the two parameters b and k.

For comparison we show in Fig. 9(a,d) the SIR-time distributions. Here definitely no enhanced asymmetry occurs. Apart from the absent $V(\tau)$ all SIR quantities vary on the same recovery reduced time scale k^{-1}. Moreover, the SIR $S(\tau)$ saturates at the finite value given by $S_\infty^{\mathrm{SIR}} = 1 - J_\infty^{\mathrm{SIR}}$, whereas the SIRV $S(\tau)$ approaches zero after infinite time.

5. Comparison of approximate with exact solutions

We have determined all model parameters such as η, k, and b, using currently available public data [15,16] for the population amount, vaccination rate, daily number of newly deceased persons. The parameters as well as the SIRV prediction are collected in Tab. 1 for various countries.

The exact numerical solution of the SIRV model is compared with the approximant for various typical choices of k and b in Fig. 8. To highlight the effect of reduced vaccination rate b, we show three cases for each k: vanishing b (SIR model), $b = b_c/5$, and $b = b_c/2$.

Preprints (www.preprints.org) | NOT PEER-REVIEWED | Posted: 30 March 2021 doi:10.20944/preprints202103.0718.v1

country α_3 code	k	a [d^{-1}]	μ [d^{-1}]	b	b/b_c	α	Δ	t_0^{II} 2020-	t_v	J_∞^{I}	$J(t_v)$	$J_\infty^{b=0}$	$J_\infty^{b=b}$	$J_\infty^{b=2b}$	$\dot{J}_{\max}$	$t_{99\%}$
ARG	0.912	0.125	0.114	0.0022	0.039	0.910	0.07	08-17	20-12-28	0.069	0.228	0.282	0.277	0.274	129	21-10-17
AUT	0.905	0.520	0.471	0.0013	0.841	0.904	0.09	07-29	20-12-26	0.008	0.128	0.191	0.182	0.177	219	21-07-29
BEL	0.896	0.551	0.494	0.0011	0.271	0.895	0.10	09-06	20-12-27	0.162	0.313	0.332	0.330	0.329	244	21-05-26
BRA	0.790	0.046	0.037	0.0099	0.202	0.780	0.19	07-05	21-01-14	0.145	0.247	0.489	0.432	0.398	86	22-09-29
CAN	0.962	1.018	0.980	0.0004	0.692	0.962	0.04	09-26	20-12-13	0.049	0.069	0.121	0.106	0.099	68	21-06-05
CHE	0.894	0.458	0.409	0.0023	1.237	0.891	0.10	07-22	21-01-22	0.044	0.216	0.240	0.236	0.234	231	21-09-05
DEU	0.915	0.559	0.511	0.0012	1.077	0.913	0.08	08-16	20-12-26	0.019	0.069	0.182	0.158	0.143	180	21-08-06
ESP	0.876	0.175	0.153	0.0046	1.120	0.871	0.12	04-29	21-01-02	0.092	0.207	0.309	0.283	0.270	115	22-01-28
FIN	0.997	3.858	3.848	0.0002	2.181	0.997	0.00	12-21	20-12-30	0.007	0.008	0.019	0.012	0.011	17	21-02-21
FRA	0.886	0.228	0.202	0.0027	0.973	0.883	0.11	05-11	20-12-26	0.082	0.183	0.284	0.263	0.252	127	21-12-25
GBR	0.867	0.389	0.337	0.0053	1.741	0.862	0.13	09-09	20-12-12	0.120	0.151	0.343	0.257	0.223	200	21-06-16
ISR	0.855	0.050	0.042	0.1283	2.518	0.727	0.00	08-20	20-12-18	0.035	0.100	0.330	0.142	0.127	62	21-09-07
ITA	0.873	0.289	0.252	0.0022	0.982	0.871	0.12	05-27	20-12-26	0.114	0.233	0.329	0.315	0.306	189	21-11-04
MEX	0.712	0.038	0.027	0.0044	0.052	0.707	0.27	07-13	20-12-23	0.123	0.234	0.586	0.559	0.535	124	22-11-23
NLD	0.929	0.397	0.369	0.0022	2.039	0.927	0.07	06-11	21-01-15	0.072	0.149	0.201	0.186	0.179	89	21-11-18
RUS	0.933	0.337	0.314	0.0008	0.423	0.933	0.07	07-22	20-12-14	0.003	0.049	0.135	0.118	0.107	74	21-10-30
SWE	0.922	0.652	0.601	0.0010	0.540	0.921	0.08	10-11	20-12-26	0.126	0.167	0.260	0.240	0.229	162	21-06-04
USA	0.868	0.218	0.189	0.0081	0.948	0.860	0.12	09-03	20-12-19	0.094	0.167	0.326	0.263	0.238	156	21-07-28

Table 1: Analysis using data from 18 Mar 2021. For η, k and a we use the current values for the 2nd wave, that started at t_0^{II}, all from an online resource, Ref. [16] The begin t_v of the vaccination program and the mean daily fraction v of vaccinated population since then we retrieve from Ref. [15], assuming that each person has to be vaccinated twice, and that the vaccination is effective two weeks after the 2nd shot. The remaining quantities are derived from Eqs. (8) and (35), i.e., via $\mu = ak$, $b = v/a$, $\alpha = k - b$, and $\Delta = 1 - 2\eta - k - b$ is positive if the outburst condition (10) is fulfilled. b_c is calculated via Eq. (91). Furthermore included are the infected population fraction at various times: (i) J_∞^{I} at the end of the first wave, $J_\infty(t_v)$ at the onset of vaccinations, (iii) $J_\infty^{b=0}$ assuming no vaccinations, (iv) $J_\infty^{b=b}$ assuming ongoing vaccination at the present rate, (v) $J_\infty^{b=2b}$ assuming the vaccination rate had been twice as large. The $t_{99\%}$ denotes the date at which 99% of the final J_∞ has been reached, and $\dot{J}_{\max} = j_{\max} a \times 10^5 / N$ is the number of newly infected persons per 100,000 inhabitants within a single day, at peak time. The difference between $J_\infty^{b=b}$ and $J_\infty^{b=0}$ is the population fraction that profits from the current vaccination program. For all countries $\eta \ll 1$, $k \in [0.7, 1]$, $\alpha \in [0.7, 1]$, $b \ll 1$ hold. A daily updated, and extended table containing more numbers such as η, v is part of the supplementary material.

Preprints (www.preprints.org) | NOT PEER-REVIEWED | Posted: 30 March 2021 doi:10.20944/preprints202103.0718.v1

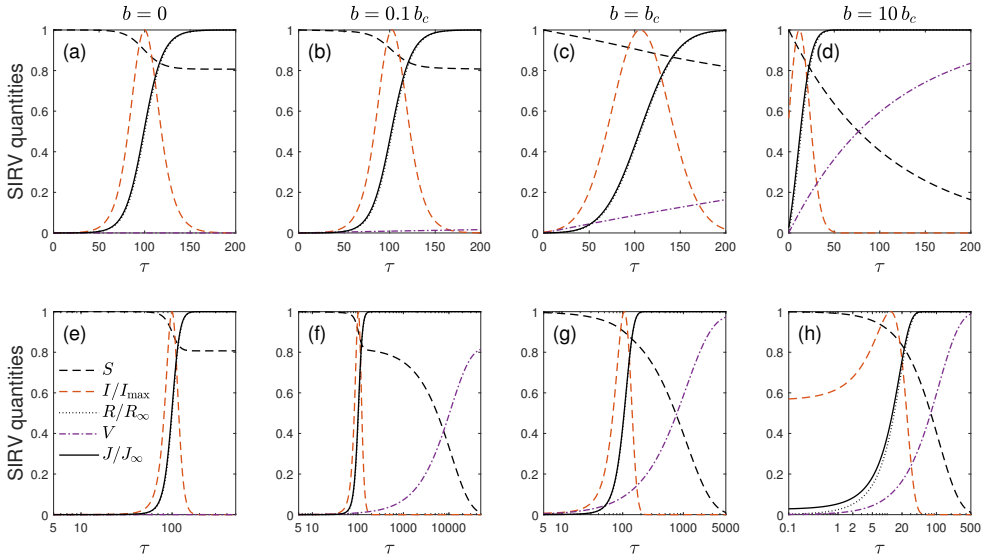

Figure 9. Suitable normalized SIRV quantities S, $I/I_{\max}$, R/R_∞, V, and J/J_∞ versus τ for four different reduced vaccination rates at $k = 0.9$ and $\eta = 10^{-6}$. (a,e) $b = 0$ (SIR model), (b,f) $b = 0.1\,b_c$, (c,g) $b = b_c$, and (d,h) $b = 10\,b_c$. While the first row presents data on a linear scale, the second row shows the same cases, but in a semilogarithmic fashion to appreciate the two well separated time scales.

These three values capture the qualitative behavior for all b. For $b \ll b_c$, vaccination is basically ineffective in reducing the number of infections. For $b \gg b_c$, the vaccination program is highly effective. The crossover is at $b = b_c$, where the reduction becomes significant, and where it depends roughly linear on b. The critical b_c as function of k and η is shown in Fig. 4. While b_c basically coincides with η for $k \to 1$, at smaller k the critical b_c behaves nonlinear with k and η, as shown.

The exact result (solid black lines) for J_∞ versus b for various k is compared with the approximant (colored lines) in Fig. 7. The gap in the colored curves marks the crossover regime, $b = b_c$. For any b, the exact solution is captured by the SIRV approximant. The same is true for remaining quantities such as peak height $j_{\max}$ and peak time $\tau^j_{\max}$, as demonstrated by Figs. 6 and 5.

6. Application to real data

To make predictions and draw conclusions from the SIRV model about the ongoing pandemic and the vaccination efforts, we have collected current values of infection, vaccination, and recovery rates, as well as population sizes, by making use of existing online resources. We then applied the SIRV model to calculate the time evolution of all the SIRV quantities, including final number of infected persons, or maximum daily number of newly infected persons. Examples are shown by Tab. 1, while a corresponding, daily updated table that includes even more characteristics of the 2nd pandemic wave is part of our supplementary material.

Besides the input parameters of the SIRV model such as the rates the table offers the dimensionless values for k, b, and $\alpha = k - b$, the criterion $\Delta = 1 - 2\eta - k - b$, the date t_v marking the beginning of the vaccination program, and various values for the final population fraction that is getting infected before all population has been either recovered or vaccinated. As long as Δ has positive values, new pandemic waves can occur. Table 1 indicates that apart from Israel this can happen in all countries considered. Only Israel has applied an high enough vaccination rate so that no further Covid-19 waves can occur. The table lists the population fraction J^{I}_∞ that had been infected up to the end of the first pandemic wave, the cumulative fraction $J_\infty(t_v)$ at the time the first person got vaccinated, the hypothetical cumulative fraction $J^{b=0}_\infty$ assuming there was no vaccination program, the

Preprints (www.preprints.org) | NOT PEER-REVIEWED | Posted: 30 March 2021 doi:10.20944/preprints202103.0718.v1

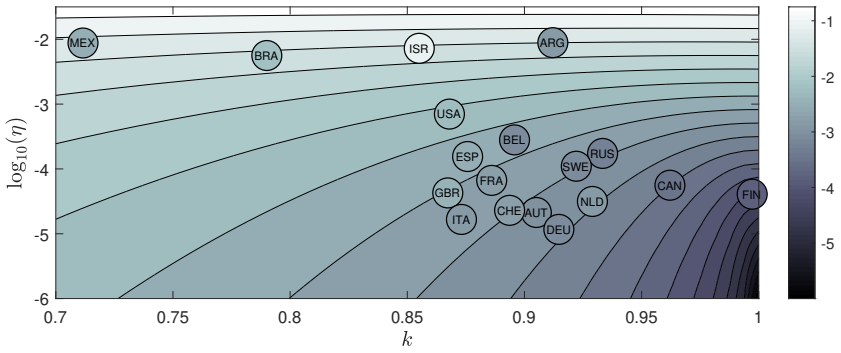

Figure 10. Same as Fig. 4 using another colormap, where countries have been added. The brightness represents $\log_{10}(b_c)$, shown as function of k and η. Circles for countries have been placed at positions k and η according to Tab. 1, and the brightness of a filled circle corresponds to the reduced vaccination rate b, again from Tab. 1.

$J_\infty = J_\infty^{b=b}$ using the current value for the mean number of vaccinated persons that gave rise to b, and the hypothetical $J_\infty^{b=2b}$ assuming vaccinations could have been performed at twice the actual speed. In addition, the table shows the maximum number of newly infected persons per day and per 100,000 inhabitants ($\dot{J}_{\max}$), and the date $t_{99\%}$ for which 99% of the ultimately infected population fraction has been reached. Note that $J_\infty^{b=2b}$ is not always much smaller than J_∞ because the vaccination program eventually started after the peak time, and because the first wave cumulative fraction J_∞^1 sets already a lower limit.

Adding the data for all countries of Tab. 1 to Fig. 4, we end up with with Fig. 10, where we have used another colormap for the purpose of this figure. The brightness represents $\log_{10}(b_c)$, shown as function of k and η. Circles for countries have been placed at positions k and η according to Tab. 1, and the brightness of a filled circle corresponds to the reduced vaccination rate b, again from Tab. 1. If the brightness of a circle exceeds the one of the background, the vaccination rate resides above the critical b_c for that country. This is the case for Israel (ISR) and Great Britain (GBR), and Finland (FIN), for example. Circles darker than background, such as for Belgium (BEL), Mexico (MEX) and Argentina (ARG), highlight cases where $b < b_c$.

7. Summary and conclusions

With the now available vaccination against COVID-19 it is quantitatively explored how vaccination campaigns influence the mathematical modeling of epidemics. For this purpose the well-known susceptible-infectious-recovered/removed (SIR) epidemic model is extended to the fourth compartment V of vaccinated persons and the vaccination rate $v(t)$ that regulates the relation between susceptible and vaccinated persons. The vaccination rate $v(t)$ competes with the infection ($a(t)$) and recovery ($\mu(t)$) rates in determining the time evolution of epidemics. In order for a pandemic outburst with rising rates of new infections it is required that $k + b < 1 - 2\eta$, where $k = \mu_0/a_0$ and $b = v_0/a_0$ denote the initial ratios of the three rates, respectively, and $\eta \ll 1$ is the initial fraction of infected persons.

Apparently for the first time we derive analytical solutions for the time-dependence of all relevant quantities $Q \in [S, I, R, V, j, J]$ of the SIRV-model where $j = \dot{J}$ and J are the daily and cumulative fraction of new infections, respectively. As in our earlier analysis of the SIR-model we eliminate one of the time-dependent rates by using the new reduced time-variable τ defined with the infection rate by $d\tau/dt = a(t)$. Moreover, we adopt the semi-time case with constant ratios $k = \mu(t)/a(t)$ and $b = v(t)/a(t)$ between the infection, recovery and vaccination rates. This assumption still allows us to account for any given time-dependence of the infection rate with the caveat that the recovery and vaccination rate have exactly the same time dependence as the infection rate apart from their different initial values. Exact analytical inverse solutions $t(Q)$ for all relevant quantities Q of the

Preprints (www.preprints.org) | NOT PEER-REVIEWED | Posted: 30 March 2021 doi:10.20944/preprints202103.0718.v1

resulting SIRV-model in terms of Lambert functions are derived. The values of the three parameters k, b and η completely determine the reduced time evolution the SIRV-quantities $Q(\tau)$.

These inverse solutions can be approximated with high accuracy yielding the explicit reduced time-dependences $Q(\tau)$ by inverting the Lambert functions. For a given time-dependence of the infection rate $a(t)$ the real time-dependence $Q(t)$ can be inferred. The inversion of the Lambert functions operates well for all ratios b exceeding a small but finite critical value b_c. In the range of $b \in [0, b_c]$ we interpolate the solution using the exact SIR-solution derived before at $b = 0$ and the inverted SIRV-solution at b_c. This approach is remarkably accurate as the comparison with the exact numerical solutions of the SIRV-equations indicates. The analytical solutions show that SIRV-pandemic waves in the relevant case $0 < b \ll \alpha < 1$ exhibit a clear asymmetric distribution in reduced and real time. The fractions of infected (I) and recovered (R) persons as well as the daily rate of new infections (j) vary rapidly on the order of the recovery reduced time scale $\tau_r \simeq \alpha^{-1} \simeq k^{-1}$. Alternatively, the fractions of susceptible (S) and vaccinated (V) persons as well as the sum $\Phi = S + I$ vary slowly on the order of the much greater vaccination reduced time scale $\tau_v \simeq b^{-1}$. This asymmetric SIRV-time behavior is significantly different from the SIR-time behavior, where no time asymmetry occurs, and, apart from the absent $V(\tau)$, all SIR quantities vary on the same recovery reduced time scale k^{-1}.

Clearly our analytical solutions are superior to all numerical ones in the literature as they allow us to identify the main determining parameters of the epidemic waves and to understand the correlations between various monitored observables. And indeed as demonstrated the three parameters b, k and η fully control the evolution of the pandemic wave in reduced time. Also valuable is the use of our exact analytical solutions as benchmark for solutions obtained by solving the SIRV-equations numerically.

The influence of vaccinations on the total cumulative number and the maximum rate of new infections in different countries is calculated by comparing our results with monitored real time Covid-19 data. The reduction in the final cumulative fraction of infected persons and in the maximum daily rate of new infections is quantitatively determined by using the actual pandemic parameters $a(0)$, k and b in different countries. The corresponding numbers for an hypothetical adopted doubled (as compared to the actual one) vaccination rate are also given which allows to quantitively assess the total and maximum casualities caused by the delayed and low-level vaccination coverage in many countries. Moreover, a new criterion is developed that decides on the occurrence of future Covid-19 waves in these countries. Apart from Israel this can happen in all countries considered. Only Israel has applied an high enough vaccination rate so that no further Covid-19 waves can occur.

Author Contributions: Both authors contributed equally to this work.

Funding: This research received no external funding.

Data Availability Statement: The data presented in this study are openly available in [16] and [15].

Conflicts of Interest: The authors declare no conflict of interest.

Appendix A Range of application for the two Lambert functions

As discussed before in Appendix G of Ref. [11] there is a single real-valued solution $W_0(y)$ of Lambert's equation for arguments $y \geq 0$, referred to as the principal. There are two real valued solutions for $y \in [-e^{-1}, 0]$: the principal one $W_0 \in [-1, 0]$ and the non-principal solution $W_{-1} \leq -1$. For arguments below $y < -e^{-1}$ only complex-valued solutions exist which are of no interest here because the function Φ is real-valued.

As the function $\Phi = I + S \in [0, 1]$ we require for the general solution (55) that

$$-\alpha W\left(-\frac{E}{\alpha}\right) \in [0, 1] \tag{A1}$$

Preprints (www.preprints.org) | NOT PEER-REVIEWED | Posted: 30 March 2021 doi:10.20944/preprints202103.0718.v1

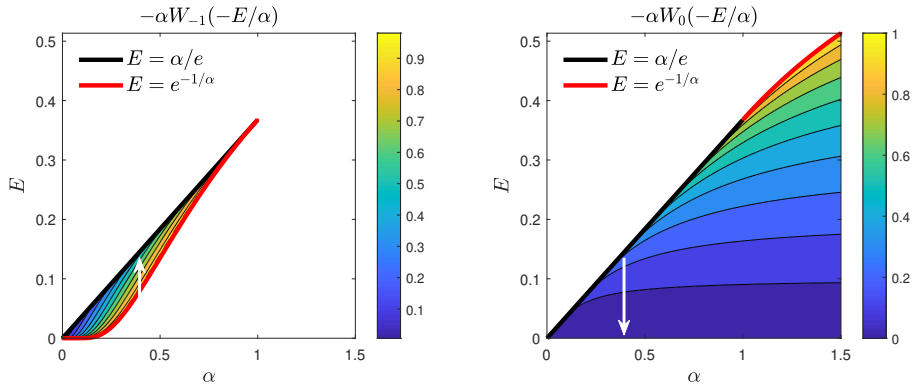

Figure A1. Values of the (**a**) non-principal and (**b**) principal Lambert functions determining Φ in Eq. (55). The solid black line represents the upper limit $E = \alpha/e = 0.368\alpha$ (for all $\alpha > 0$), where $\Phi = \alpha$. Only for the coloured region below this line real-valued solutions of Eq. (55) exist. The red line represents the initial $E(\psi_0)$, which serves as a more restrictive upper limit for $\alpha > 1$. In their coloured areas the corresponding Lambert functions apply, while the white regions cannot be reached. Points residing in (α, E)-space that are shared by both Lambert functions are visited at different times, as exemplarily shown by the white arrows for $\alpha = 0.25$. At early times the non-principal Lambert function W_{-1} describes Φ, while W_0 overtakes at later times. The crossover occurs at $\Phi = \alpha$. At this moment, both Lambert function exhibit exactly the same value. For negative $\alpha < 0$, the accessible E span the huge range $E \in [0, e^{-1/\alpha}]$ and are therefore not shown. For such $\alpha < 0$, the colored region exists only for W_0.

with the always positive $E > 0$. While for $\alpha < 0$ the only real-valued Lambert function is W_0, for values $\alpha > 0$ of particular interest here the argument of the Lambert function is always negative. For those α's, real-valued solutions exist only if

$$E \leq \frac{\alpha}{e} \simeq 0.368\alpha \tag{A2}$$

In Fig. A1 we plot the two functions $-\alpha W_0(-E/\alpha)$ and $-\alpha W_{-1}(-E/\alpha)$ entering the constraint (A1). The black line represents the upper limit (A2) and the red line represents the initial $E(\psi_0) = e^{-1/\alpha}$. For $\alpha \notin [0, 1]$ the initial value provides a more restrictive upper limit for E, as E is monotonically decreasing in those cases, as we have proven already.

The lower bound of the constraint (A1) is automatically fulfilled for all negative arguments of the Lambert function. The principal Lambert function applies for $-1 \leq W_0(-E/\alpha) \leq 0$, corresponding to the range

$$-\alpha W_0\left(-\frac{E}{\alpha}\right) \in [0, \alpha] \tag{A3}$$

which automatically fulfils the upper bound of the constraint (A1) when $\alpha < 1$ is smaller than unity. The coloured area in the Fig. A1b represents the constraint (53). When $\alpha > 1$ or $\alpha < 0$, the constraint (A1) is still fulfilled as long as $E \leq e^{-1/\alpha}$, as this value for E inserted into Eq. (A1) gives unity. As we had already shown, ψ monotonically increases (decreases) with time τ for $\alpha > 1$ ($\alpha < 0$), $E(\psi)$ varies monotonically with ψ, and $E_\infty = 0$. The $E(\psi)$ therefore monotonically decreases with time for both $\alpha > 1$ and $\alpha < 0$, and thus stays below $e^{-1/\alpha}$ at all times, since $E(\psi_0) = e^{-1/\alpha}$. The constraint (A1) is therefore not only fulfilled automatically for $\alpha \in (0, 1)$, but for all α. The only exception from this statement are $\alpha = 0$ and $\alpha = 1$, as we have not discussed these special cases here.

Likewise, the non-principal Lambert function potentially applies for $W_{-1}(-E/\alpha) < -1$, corresponding to the range $-\alpha W_{-1}(-E/\alpha) > \alpha$. Together with the right-hand side of the constraint (A1) we find that the non-principal solution potentially applies as solution

Preprints (www.preprints.org) | NOT PEER-REVIEWED | Posted: 30 March 2021 doi:10.20944/preprints202103.0718.v1

k	$\log_{10}(b_c^{\rm fit})$	$\log_{10}(b_c)$	$\log_{10}(b_c^\dagger)$
0.100	−1.18	−1.19	−1.18
0.300	−1.44	−1.44	−1.53
0.500	−1.75	−1.74	−1.88
0.650	−2.06	−2.05	−2.25
0.800	−2.51	−2.50	−2.77
0.850	−2.74	−2.73	−3.03
0.900	−3.05	−3.04	−3.39
0.950	−3.56	−3.57	−4.00
0.980	−4.21	−4.23	−4.80
0.990	−4.69	−4.70	−5.41
0.995	−5.13	−5.13	−6.01

Table 2: Critical value b_c of the reduced vaccination rate b to be used in the interpolants (100) and (102). Mentioned for comparison: The best fitted value $b_c^{\rm fit}$, the analytic expression (91) for b_c that is used throughout this work, and the rough estimate $b_c^\dagger$ according to Eq. (A6). This table is for $\eta = 10^{-6}$, the analytic expression (91) works equally well for any $\eta \ll 1$.

in the range

$$-\alpha W_{-1}\left(-\frac{E}{\alpha}\right) \in [\alpha, 1] \tag{A4}$$

The coloured area in Fig. A1a represents the constraint (A4). It is not obvious at first glance why there are regions in α–E-space that fulfill both inequalities (A3) and (A4). In those regions only one of the two Lambert functions can lead to the true Φ. The transition between the two Lambert functions is where they meet, i.e., when $\Phi = \alpha$. When $\alpha \in (0, 1)$, the Φ at early times involves W_{-1}. This continues until a point in time where $\Phi = \alpha$ is reached. From then on, Φ is determined by the principal solution W_0.

Appendix B The critical vaccination rate b_c

It is straightforward to estimate the value b_c of the parameter b, below which the approximations (80) and (82) break down. This occurs when the approximation in Eq. (65), based on the assumption of values of $\psi \gg 1$ is no longer valid, i.e. when the minimum ψ_m given by Eq. (73) exceeds a certain value of order unity. Consequently, the approximation tends to break down if the following equation is fulfilled for b_c

$$1 = \psi_0 - \frac{1 - (k - b_c) + (k - b_c)\ln(k - b_c)}{b_c} \tag{A5}$$

Introducing an abbreviation for $k - b_c$ this equation can be cast into the form of the Lambert equation (51) with the solution

$$b_c^\dagger \;=\; k - e^{2-\psi_0} \exp\left\{ W_0\left[-\frac{(1 + k - k\psi_0)}{e^{2-\psi_0}} \right] \right\} \tag{A6}$$

in terms of the principal Lambert function. The solution we have denoted here by $b^\dagger$, as the b_c to be used will be slightly different, as shown below. The non-principal Lambert function would produce large b_c values for which our approximants do not require any special treatment. Using $\psi_0 = \ln[(1 - \eta)/\eta]$, the expression (A6) may be rewritten further. Different choices of the left hand side of Eq. (A5) give slightly different values for $b_c^\dagger$. It is important to note that our approximants for the regime $b < b_c$ cannot be evaluated anymore for values well below $b_c^\dagger$, especially for k very close to unity. In Tab. 2 we therefore collect best values for b_c, that we obtained upon fitting the exact solution with our approximant, and compare them with the formula (A6) as well as with another formula to be derived next, that will actually be used as it captures the best b_c with much higher accuracy than $b_c^\dagger$.

Preprints (www.preprints.org) | NOT PEER-REVIEWED | Posted: 30 March 2021 doi:10.20944/preprints202103.0718.v1

Upon inspecting the fitted b_c for various k and η we find that one has $b_c \ll 1$, $J_\infty(k, b_c) \gg \eta$, and a constant proportionality between J_∞ and $b_c^{1/3}$. In light of Eq. (A15) this translates into the following equation for b_c

$$\sqrt{\frac{k}{b_c}}\, e^{\frac{1-k+k\ln k}{b_c}} = \frac{b_c^{1/3}}{\eta\sqrt{c}} \tag{A7}$$

with some coefficient $c = 32\pi$ which we determine empirically (Fig. 2) upon comparing the exact solution with the approximant. This Eq. (A7) is solved for b_c as follows

$$b_c = \left(32\pi k\eta^2\right)^{3/5} \exp\left\{W_0\left[\frac{6(1-k+k\ln k)}{5(32\pi k\eta^2)^{3/5}}\right]\right\} \tag{A8}$$

This final expression for b_c is compared with the fitted b_c and the above estimate $b_c^\dagger$ in Tab. 2. The agreement between fitted and analytic b_c is excellent for all η and k.

Appendix C Proof of Eq. (71)

Here we prove that $W_0(z(\psi_0)) = -1/\alpha$ for all $\alpha \notin [0, 1)$, where we recall that $z(\psi_0) = -e^{-1/\alpha}/\alpha$. This identity was used in the derivation of Eq. (71). Making use of the inverse Lambert function $W_0^{-1}(w) = we^w$, we can take the inverse on both sides

$$z(\psi_0) = -\frac{e^{-1/\alpha}}{\alpha} = W_0^{-1}\left(-\frac{1}{\alpha}\right) = -\frac{1}{\alpha}e^{-1/\alpha} \tag{A9}$$

which completes the proof, but one has to be careful here. The identity holds only for those α for which $W_0(z)$ resides on its real-valued regime, i.e., $W_0 \in [-1, \infty]$ for $z \in [-e^{-1}, \infty]$. Because the argument $-\alpha^{-1}$ of the inverse Lambert function is ≥ -1 only for $\alpha < 0$ and $\alpha \geq 1$, the identity does not hold for $\alpha \in [0, 1)$. If W_0 is replaced by W_{-1}, the identity holds for the opposite case of $\alpha \in (0, 1]$.

Appendix D Proofs of Eqs. (101) and (102)

With the approximate expression (94) that is useful up to order $\mathcal{O}(\eta^2)$ we obtain for corresponding cumulative number fraction with the substitution $\xi = e^{-b\tau'}/b$

$$\begin{aligned} J(\tau) &= J(0) + \int_0^\tau j(\tau')\, d\tau' \\ &= \eta\left\{1 + b^{\frac{k}{b}} e^{\frac{1}{b}} \int_{\frac{e^{-b\tau}}{b}}^{\frac{1}{b}} \xi^{\frac{k}{b}} e^{-\xi} d\xi\right\} \\ &= \eta\left\{1 + b^{\frac{k}{b}} e^{\frac{1}{b}} \left[\gamma\left(1 + \frac{k}{b}, \frac{1}{b}\right) - \gamma\left(1 + \frac{k}{b}, \frac{e^{-b\tau}}{b}\right)\right]\right\} \end{aligned} \tag{A10}$$

where we have inserted $J(0) = \eta$ and used the lower incomplete gamma function [12] defined by

$$\gamma(s, x) = \int_0^x \xi^{s-1} e^{-\xi}\, d\xi \tag{A11}$$

After infinite time we readily obtain from (A10)

$$J_\infty(k, b) = \eta\left[1 + b^{\frac{k}{b}} e^{\frac{1}{b}} \gamma\left(1 + \frac{k}{b}, \frac{1}{b}\right)\right] = \eta k b^{\frac{k}{b}-1} e^{\frac{1}{b}} \gamma\left(\frac{k}{b}, \frac{1}{b}\right),$$

Preprints (www.preprints.org) | NOT PEER-REVIEWED | Posted: 30 March 2021 doi:10.20944/preprints202103.0718.v1

where in the last step we used the recurrence formula [12] $\gamma(1+s,x) = s\gamma(s,x) - x^s e^{-x}$ for $s = k/b$ and $x = 1/b$. For the special case of $k = b$ this expression (A12) indeed reproduces Eq. (A53) up to order $\mathcal{O}(\eta^2)$, i.e.

$$J_\infty(k,k) = \eta k(e^{1/k} - 1) \tag{A12}$$

where we used $\gamma(1,x) = 1 - e^{-x}$. For the special case of $k = 0$, Eq. (A12) simplifies to

$$J_\infty(0,b) = e^{1/b}\eta \tag{A13}$$

As already discussed, the Eq. (A12) is useful when b does not exceed b_c. This avoids that the latter expression (A13) exceeds unity and thus fails when b is too small.

With the asymptotic behavior of the gamma function

$$\gamma(s, x \gg 1) \simeq \Gamma(s) - x^{s-1}e^{-x} \simeq \Gamma(s) \tag{A14}$$

we obtain from Eq. (A12) for small values of $b \ll 1$

$$J_\infty(k, b \ll 1) \simeq \eta k b^{\frac{k}{b}-1} e^{\frac{1}{b}} \Gamma\left(\frac{k}{b}\right) \simeq \eta\sqrt{\frac{2\pi k}{b}} e^{\frac{1-k+k\ln k}{b}} \tag{A15}$$

where we used Stirling's formula $\Gamma(s \gg 1) \simeq (2\pi)^{1/2} s^{s-\frac{1}{2}} e^{-s}$ in the last step.

Appendix E Cumulative fraction of infected persons $J(\tau)$ for arbitrary η

Starting from our approximants for $S(\tau)$ and $I(\tau)$ given by Eq. (27), with $\psi(\tau)$ from Eq. (26), i.e.,

$$\psi(\tau) = \psi_0 + \alpha\tau - \frac{1 - e^{-b\tau}}{b},\ \alpha = k - b \tag{A16}$$

the differential rate $j(\tau) = S(\tau)I(\tau)$ (29) is written as

$$j(\tau) = \frac{e^{-2b\tau}}{4\cosh^2\frac{\psi}{2}} = \frac{e^{-2b\tau-\psi(\tau)}}{(1+e^{-\psi})^2} = \frac{e^{\psi(\tau)-2b\tau}}{(1+e^{\psi})^2}. \tag{A17}$$

Here we are interested in an expression for the integrated $j(\tau)$ for arbitrary initial conditions η, contained in $\psi_0 = \ln[(1-\eta)/\eta]$, while a result valid for small $\eta \ll 1$ we have already provided with Eq. (A10). To this end we calculate with Eqs. (30) and (A17)

$$\begin{aligned} J(\tau) &= \eta + \int_0^\tau d\tau' j(\tau') \\ &= \eta + \int_0^\tau d\tau' \frac{e^{-2b\tau'-\psi(\tau')}}{(1+e^{-\psi(\tau')})^2} \\ &= \eta + \int_0^\tau d\tau' \frac{e^{-[\psi_0+(2b+\alpha)\tau' - \frac{1-e^{-b\tau'}}{b}]}}{(1+e^{-[\psi_0+\alpha\tau' - \frac{1-e^{-b\tau'}}{b}]})^2} \end{aligned} \tag{A18}$$

Substituting $\xi = e^{-b\tau'}/b$ then yields

$$J(\tau) = \eta + \int_{\frac{e^{-b\tau}}{b}}^{\frac{1}{b}} d\xi \frac{(b\xi)^{\frac{\alpha}{b}+1} e^{\frac{1}{b}-\psi_0-\xi}}{[1+(b\xi)^{\frac{\alpha}{b}} e^{\frac{1}{b}-\psi_0-\xi}]^2} \tag{A19}$$

To be able to calculate this integral we introduce yet another, but simpler integral $U(c)$ parameterized by c,

$$U(c) = c\eta + b\int_{\frac{e^{-b\tau}}{b}}^{\frac{1}{b}} \frac{d\xi}{1 + e^{\frac{1}{b}-\psi_0}(b\xi)^{\frac{\alpha}{b}} e^{-c\xi}} \tag{A20}$$

Preprints (www.preprints.org) | NOT PEER-REVIEWED | Posted: 30 March 2021 doi:10.20944/preprints202103.0718.v1

Because the derivative of $U(c)$ with respect to c evaluates to

$$\frac{dU(c)}{dc} = \eta + \int_{\frac{e^{-b\tau}}{b}}^{\frac{1}{b}} d\xi \frac{e^{\frac{1}{b}-\psi_0}(b\xi)^{\frac{\alpha}{b}+1}e^{-c\xi}}{(1+e^{\frac{1}{b}-\psi_0}(b\xi)^{\frac{\alpha}{b}}e^{-c\xi})^2} \tag{A21}$$

we can express the cumulative fraction (A19) in terms of $U(c)$ as

$$J(\tau) = \left.\frac{dU}{dc}\right|_{c=1} \tag{A22}$$

We are left to calculate the integral (A20). Using the identity

$$\frac{1}{1+e^{-x}} = \sum_{n=0}^{\infty}(-1)^n e^{-nx} \tag{A23}$$

applied to Eq. (A20) provides

$$\begin{aligned} U(c) &= c\eta + \sum_{n=0}^{\infty}(-1)^n e^{\frac{n}{b}-n\psi_0} b^{\frac{n\alpha}{b}+1} \int_{\frac{e^{-b\tau}}{b}}^{\frac{1}{b}} d\xi\, \xi^{\frac{n\alpha}{b}} e^{-cn\xi} \\ &= c\eta + 1 - e^{-b\tau} + \sum_{n=1}^{\infty}(-1)^n e^{\frac{n}{b}-n\psi_0}\left(\frac{b}{n}\right)^{\frac{n\alpha}{b}+1} \int_{\frac{ne^{-b\tau}}{b}}^{\frac{n}{b}} dz\, z^{\frac{n\alpha}{b}} e^{-cz}, \end{aligned} \tag{A24}$$

where we substituted $z = n\xi$ in the last step. Eq. (A24) readily yields, upon replacing τ_0, and using the Binomials $B_{m,n} = m!/[n!(m-n)!]$,

$$\begin{aligned} J(\tau) &= \left.\frac{dU(c)}{dc}\right|_{c=1} = \eta + \sum_{n=1}^{\infty} e^{-n\psi_0} J_n(\tau) \\ &= \eta + \sum_{n=1}^{\infty}\left(\frac{\eta}{1-\eta}\right)^n J_n(\tau) \\ &= \eta + \sum_{m=1}^{\infty}\left[\sum_{n=1}^{m} B_{m-1,n-1} J_n(\tau)\right]\eta^m \end{aligned} \tag{A25}$$

with the coefficients

$$J_n(\tau) = (-1)^{n+1} e^{\frac{n}{b}}\left(\frac{b}{n}\right)^{\frac{n\alpha}{b}+1} \int_{\frac{ne^{-b\tau}}{b}}^{\frac{n}{b}} dz\, z^{\frac{n\alpha}{b}+1} e^{-z} \tag{A26}$$

that all vanish for $\tau = 0$. We have kept the exponential weight containing ψ_0 in front of the coefficient $J_n(\tau)$ in Eq. (A25) as this allowed us to see that we need to take into account the first m terms of the sum, and the first m coefficients J_m to come up with $J(\tau)$ up to order $O(\eta^m)$. The integral in the coefficient can be expressed in terms of the lower incomplete gamma function γ so that we finally have obtained $J(\tau)$ as infinite sum, whose summands are given by

$$J_n(\tau) = (-1)^{n+1} e^{\frac{n}{b}}\left(\frac{b}{n}\right)^{\frac{n\alpha}{b}+1} \times \left[\gamma\left(\frac{n\alpha}{b}+2, \frac{n}{b}\right) - \gamma\left(\frac{n\alpha}{b}+2, \frac{ne^{-b\tau}}{b}\right)\right] \tag{A27}$$

Preprints (www.preprints.org) | NOT PEER-REVIEWED | Posted: 30 March 2021 doi:10.20944/preprints202103.0718.v1

To confirm that our general expression reduces to the one (A10) we had already derived for small $\eta \ll 1$, we evaluate Eq. (A25) to first order in η. With $B_{0,0} = 1$ the Eq. (A25) implies

$$\begin{aligned} J(\tau) &\simeq \eta + J_1(\tau)\eta \\ &= \eta + \eta e^{\frac{1}{b}} b^{\frac{\alpha}{b}+1} \left[\gamma\left(\frac{\alpha}{b}+2, \frac{1}{b}\right) - \gamma\left(\frac{\alpha}{b}+2, \frac{e^{-b\tau}}{b}\right)\right] \\ &= \eta\left\{1 + e^{\frac{1}{b}} b^{\frac{k}{b}} \left[\gamma\left(1+\frac{k}{b}, \frac{1}{b}\right) - \gamma\left(1+\frac{k}{b}, \frac{e^{-b\tau}}{b}\right)\right]\right\} \end{aligned} \tag{A28}$$

where we have taken J_1 from Eq. (A27), and replaced α by $k - b$. This Eq. (A28) is indeed identical to Eq. (A10).

We can rewrite $J(\tau)$ further in a way that helps calculating $J_\infty = \lim_{\tau\to\infty} J(\tau)$ using the recurrence formula for the lower incomplete gamma function,

$$\gamma(a+1, x) = a\gamma(a, x) - x^a e^{-x} \tag{A29}$$

Using this recurrence in the first line of Eq. (A25), we end up with

$$\begin{aligned} J(\tau) &= \frac{1}{e^{b\tau} + e^{\psi_0 + k\tau - \frac{1-e^{-b\tau}}{b}}} \\ &\quad + \sum_{n=1}^{\infty} (-1)^{n+1} \chi_n e^{\frac{n}{b} - n\psi_0} \left(\frac{b}{n}\right)^{\chi_n} \times \left[\gamma\left(\chi_n, \frac{n}{b}\right) - \gamma\left(\chi_n, \frac{ne^{-b\tau}}{b}\right)\right] \end{aligned} \tag{A30}$$

where we have used the abbreviation

$$\chi_n = 1 + \frac{n\alpha}{b} \tag{A31}$$

only to shorten the expression. Note that $\chi_1 = k/b$. To derive this expression (A30) we made use of the following identities,

$$\sum_{n=1}^{\infty} (-1)^n e^{-nx} = -\frac{1}{1+e^x} \tag{A32}$$

as well as

$$\sum_{n=1}^{\infty} (-1)^{n+1} e^{-n\psi_0} = \sum_{n=1}^{\infty} (-1)^{n+1} e^{-n\psi_0} = \frac{1}{1+e^{\psi_0}} = \eta \tag{A33}$$

After infinite time the first term of Eq. (A30) vanishes, and $\gamma(\chi_n, 0) = 0$ can be used. Hence

$$J_\infty = \sum_{n=1}^{\infty} (-1)^{n+1} \chi_n e^{\frac{n}{b} - n\psi_0} \left(\frac{b}{n}\right)^{\chi_n} \gamma\left(\chi_n, \frac{n}{b}\right) \tag{A34}$$

Preprints (www.preprints.org) | NOT PEER-REVIEWED | Posted: 30 March 2021 doi:10.20944/preprints202103.0718.v1

While this appears as a tractable expression, it cannot be directly evaluated numerically for small b such as $b = b_c$, because $e^{n/b}$ poses a problem. To circumvent this problem, we make use of Stirling's formula and $\gamma(\chi_n, \infty) = \Gamma(\chi_n)$. For small values of b we then obtain

$$\begin{aligned} J_\infty^{b\ll 1} &\simeq \sum_{n=1}^{\infty} (-1)^{n+1} \chi_n e^{\frac{n}{b} - n\psi_0} \left(\frac{b}{n}\right)^{\chi_n} \Gamma(\chi_n) \\ &= \sum_{n=1}^{\infty} (-1)^{n+1} \chi_n e^{\frac{n}{b} - n\psi_0} \left(\frac{n\alpha}{b}\right) \left(\frac{b}{n}\right)^{\chi_n} \Gamma\left(\frac{n\alpha}{b}\right) \\ &\simeq \sqrt{2\pi b\alpha} \sum_{n=1}^{\infty} \frac{(-1)^{n+1} \chi_n \alpha^{\frac{n\alpha}{b}} e^{-n[\psi_0 + \frac{\alpha-1}{b}]}}{\sqrt{n}} \end{aligned} \tag{A35}$$

where eventually we re-inserted χ_n from Eq. (A31). For small values of $\eta \ll 1$ we only take the first term in this sum providing with $\alpha = k - b \simeq k$

$$J_\infty^{b\ll 1, \eta \ll 1} \simeq \eta \sqrt{2\pi b\alpha} \frac{k}{b} \alpha^{\frac{k}{b} - 1} e^{\frac{1-\alpha}{b}} = \eta \sqrt{\frac{2\pi k}{b}} e^{\frac{1 - k + k \ln k}{b}} \tag{A36}$$

which agrees exactly with Eq. (A15). It is worthwhile noticing that for very small $b \ll 1$ the higher order terms in the sum must be taken into account, even at small η, as they make sure that J_∞ stays below unity. We need to calculate J_∞ only down to $b = b_c$, while the form (91) for b_c ensures that $J_\infty < 1$.

Appendix F Peak time and amplitude for $b \geq b_c$ and arbitrary η

Our approximant $j(\tau)$, valid for $b \geq b_c$, and given by Eq. (A17) can be written as

$$j(\tau) = e^A b^2 F(x), \qquad F(x) = \frac{x^{2+p} e^{-x}}{(1 + e^A x^p e^{-x})^2} \tag{A37}$$

with $p = \alpha/b$, $e^A = e^{-\psi_0} e^{1/b} b^p = \eta e^{1/b} b^p / (1 - \eta)$, and $x = e^{-b\tau}/b$, so that $F(x)$ contains the dependency on time τ via x. Note that x is positive at all times, because b is positive. Because x varies monotonically with τ, to find the peak time $\tau_{\max}^j$, and peak height $j_{\max}$, we need to determine the position and value of $F(x)$ at its maximum, provided such maximum exists. For the derivative of $F(x)$ with respect to x one has

$$F'(x) = \frac{e^x x^{1+p} [(2 + p - x) e^x + e^A x^p (2 - p + x)}{[e^2 + e^A x^p]^3} \tag{A38}$$

The derivative hence vanishes at $x = x_{\max}$, where $x_{\max}$ solves the highly nonlinear

$$\frac{e^{x_{\max} - A}}{x_{\max}^p} = \frac{p - x_{\max} - 2}{p - x_{\max} + 2} \tag{A39}$$

or equivalently, and more suitable for any numerical implementation

$$x_{\max} - A - p \ln(x_{\max}) = \ln\left(\frac{p - x_{\max} - 2}{p - x_{\max} + 2}\right) \tag{A40}$$

Inserting Eq. (A40) into Eq. (A37) then provides for the differential rate at peak time

$$j_{\max} = j(x_{\max}) = \left(\frac{b x_{\max}}{2}\right)^2 \left[1 - \left(\frac{2}{p - x_{\max}}\right)^2\right] \tag{A41}$$

This is an expression valid for arbitrary η and $b \geq b_c$ in terms of the solution $x_{\max}$ of Eq. (A40), that can only be obtained numerically. For the special case of small $b \ll k$, we can proceed analytically and provide an approximate solution for $x_{\max}$.

Preprints (www.preprints.org) | NOT PEER-REVIEWED | Posted: 30 March 2021 doi:10.20944/preprints202103.0718.v1

Appendix F.1 Special case of $b_c \leq b \ll k$

For this relevant case or small $b \ll k$, the above p becomes large and well approximated by $p \simeq k/b$. At the same time does the right hand side of Eq. (A40) vanish. The remaining equation for $x_{\max}$,

$$x_{\max}^{p} e^{-x_{\max}} = e^{-A} \tag{A42}$$

is solved with the help of Lambert's principal function as

$$x_{\max} = -\frac{\alpha}{b} W_0\left(-\frac{e^{-A/p}}{p}\right) = -\frac{\alpha}{b} W_0\left(-\frac{e^{-\frac{(1-b\psi_0)}{\alpha}}}{\alpha}\right) \tag{A43}$$

where we have replaced p and used properties of the Lambert function. The corresponding $j_{\max}$ is still given by Eq. (A41). Because ψ_0 is of order unity, and if $b\psi_0 \ll 1$ holds as well, the argument of W_0 simplifies for $b \ll k$ to $-e^{-1/k}/k$. This latter argument equals $-e^{-1}$ to within 2.5% for all $k \in [0.8, 1]$, so that $x_{\max} \simeq \alpha/b = p$, and equivalently, $\tau_{\max} \simeq -\ln(\alpha)/b$ can be used under such circumstances.

Appendix G Exact solutions for special cases

Appendix G.1 The equal value case $b = k$ corresponding to $\alpha = 0$

Our general analysis above can also be used for a number of special cases to be investigated in this and the next appendices. We start with the special case $\alpha = 0$ the general Eqs. (36) and (46) simplify to

$$\Phi = -\frac{d\psi}{d\tau} = 1 + k(\psi - \psi_0) \tag{A44}$$

With the initial condition $\psi(0) = \psi_0$ Eq. (A44) immediately integrates to

$$\psi(\tau) = \psi_0 + \frac{e^{-k\tau} - 1}{k}, \tag{A45}$$

implying

$$\Phi(\tau) = I(\tau) + S(\tau) = -\frac{d\psi}{d\tau} = e^{-k\tau} \tag{A46}$$

This proves that our Eq. (79) is actually exact, and not an approximant, for this special case of $\alpha = 0$. With Eqs. (A45)–(A46) we readily obtain for Eqs. (47)–(48)

$$I(\tau) = \frac{e^{-k\tau}}{1+e^{\psi}} = \frac{e^{-k\tau}}{2}\left[1 - \tanh\frac{\psi}{2}\right] = \frac{e^{-k\tau}}{1+\exp[\psi_0 - \frac{1-e^{-k\tau}}{k}]}, \tag{A47}$$

$$S(\tau) = \frac{e^{-k\tau}}{1+e^{-\psi}} = \frac{e^{-k\tau}}{2}\left[1 + \tanh\frac{\psi}{2}\right] = \frac{e^{-k\tau}}{1+\exp[\frac{1-e^{-k\tau}}{k} - \psi_0]} \tag{A48}$$

Consequently, the rate of new infections is then given by

$$j(\tau) = S(\tau)I(\tau) = \frac{e^{-2k\tau+\psi(\tau)}}{(1+e^{\psi})^2} = \frac{1}{4e^{2k\tau}\cosh^2\left(\frac{1-e^{-k\tau}}{2k} - \frac{\psi_0}{2}\right)} \tag{A49}$$

Using Eq. (50) and Φ from Eq. (A46) the $V(\tau)$ is written in terms of ψ as

$$V(\tau) = -k\ln[\eta(1+e^{\psi})] \tag{A50}$$

Because $I(\tau) + S(\tau) = 1 - R(\tau) - V(\tau)$ due to the sum constraint, the remaining $R(\tau)$ is given by

$$R(\tau) = 1 - e^{-k\tau} + k\ln[\eta(1+e^{\psi})] \tag{A51}$$

Preprints (www.preprints.org) | NOT PEER-REVIEWED | Posted: 30 March 2021 doi:10.20944/preprints202103.0718.v1

With $J(\tau) = I(\tau) + R(\tau)$ there is no need to integrate the $j(\tau)$ to come up with a final expression for $J(\tau)$ using $I(\tau)$ and $R(\tau)$ from Eqs. (A47) and (A51).

At infinite time $\tau = \infty$, we find from Eqs. (A45), (A47), and (A48)

$$\psi_\infty(k,k) = \psi_0 - \frac{1}{k}, \tag{A52}$$

as well as $I_\infty = S_\infty = j_\infty = 0$, $R_\infty + V_\infty = 1$ and $J_\infty = R_\infty$. The only nontrivial quantity is thus J_∞, which we obtain from Eq. (A52) inserted into Eq. (A51) as

$$\begin{aligned} J_\infty(k,k) &= 1 + k\ln\left\{\eta\left[1 + e^{\psi_0 - (1/k)}\right]\right\} \\ &= k\ln\eta + k\psi_0 + k\ln(1 + e^{\frac{1}{k} - \psi_0}) \\ &= k\ln(1-\eta) + k\ln(1 + e^{\frac{1}{k} - \psi_0}) \end{aligned} \tag{A53}$$

For small values of k, $J_\infty \simeq 1 + k\ln\eta$ which for $k = 0$ correctly provides $J_\infty = 1$. All other expressions can also be readily evaluated in this limit with the help of $\lim_{k\to 0}[1 - e^{-k\tau}]/k = \tau$. For $\alpha = k = b = 0$, we thus have $\psi(\tau) = \psi_0 - \tau$ and $\Phi(\tau) = 1$ and all above expressions simplify considerably. For example,

$$J_{k=0}(\tau) = \frac{1}{2}\left[1 + \tanh\frac{\tau - \psi_0}{2}\right] \tag{A54}$$

This completes the analysis of the special case of equal values of $b = k$, or equivalently, $\alpha = 0$. The most noteworthy result is the significant reduction in the final cumulative number of new infections with increasing values of $k = b$ as compared to the SI-case with $k = b = 0$, cf. Eq. (A61).

Appendix G.2 SIR-case $b = 0$, $k > 0$

For no vaccination campaigns ($b = 0$) the SIRV-model reduces to the SIR-model analyzed before [2,3]. For $b = 0$ implying $\alpha = k \geq 0$ the Eq. (46) simplifies to

$$\Phi - k\ln\Phi + k\ln(1 + e^{-\psi}) = 1 - k\ln(1-\eta), \tag{A55}$$

or with $\Phi = I + S$ and Eq. (47)

$$I + S - k\ln S = 1 - k\ln(1-\eta) \tag{A56}$$

For $b = 0$ Eq. (16) simplifies to $I = -d\ln S/d\tau$, so that Eq. (A56) becomes

$$-\frac{d\ln S}{d\tau} + S - k\ln S = 1 - k\ln(1-\eta) \tag{A57}$$

In terms of the positively valued function $G = -\ln(S)$ the Eq. (A57) reads

$$\frac{dG}{d\tau} = 1 - e^{-G} - kG - k\ln(1-\eta), \tag{A58}$$

which agrees exactly with the integrable Eq. (24) in Ref. [3] yielding

$$I(\tau) = \frac{dG}{d\tau}, \qquad S(\tau) = e^{-G} \tag{A59}$$

and for the rate of new infections j and the corresponding cumulative number J

$$j(\tau) = SI = \frac{de^{-G}}{d\tau}, \quad J(\tau) = 1 - e^{-G} \tag{A60}$$

Preprints (www.preprints.org) | NOT PEER-REVIEWED | Posted: 30 March 2021 doi:10.20944/preprints202103.0718.v1

To summarize, one finds [3] for the SIR model, the special case of the SIRV model with $b = 0$,

$$J_{\infty}^{\mathrm{SIR}} = 1 + kW_0\left(\frac{1-\eta}{ke^{\frac{1}{k}}}\right), \tag{A61}$$

$$j_{\max}^{\mathrm{SIR}} = \frac{k^2}{4}\left(\left[1 + W_{-1}\left(\frac{2(1-\eta)}{ke^{\frac{1}{k}+1}}\right)\right]^2 - 1\right) \tag{A62}$$

Appendix G.2.1 Alternative inverse solution

For $b = 0$ one obtains $\alpha = k$, so that Eq. (36) reads

$$\frac{d\psi}{d\tau} = k - \Phi \tag{A63}$$

Likewise, the general solution (55) reduces to

$$\Phi = -kW\left(-\frac{E_0(\psi)}{k}\right) \tag{A64}$$

with the positive expression

$$E_0(\psi) = \eta(1+e^{-\psi})e^{\psi_0 - \frac{1}{k}} = (1-\eta)e^{-\frac{1}{k}}(1+e^{-\psi}) \geq 0, \tag{A65}$$

Inserting the solution (A64) then provides for Eq. (A63)

$$\frac{d\psi}{d\tau} = k\left[1 + W\left(-\frac{E_0(\psi)}{k}\right)\right], \tag{A66}$$

which with the initial condition (33) readily integrates to the inverse exact solution

$$\tau = \frac{1}{k}\int_{\psi_0}^{\psi} \frac{dx}{1 + W\left(-\frac{E_0(x)}{k}\right)} \tag{A67}$$

Hence practically all previous general results obtained in Sect. III and IV also hold here with α replaced by k. For values of $k \in (0,1)$, Eq. (A67) yields

$$\tau = \tau_m + \begin{cases} \frac{1}{k}\int_{\psi_m}^{\psi} \frac{dx}{1+W_{-1}(-\frac{E_0(x)}{k})}, & \psi \leq \psi_m \\ \frac{1}{k}\int_{\psi_m}^{\psi} \frac{dx}{1+W_0(-\frac{E_0(x)}{k})}, & \psi \geq \psi_m \end{cases} \tag{A68}$$

where the time where the minimum ψ_m occurs, is given by

$$\tau_m = \frac{1}{k}\int_{\psi_0}^{\psi_m} \frac{dx}{1 + W_{-1}\left(-\frac{E_0(x)}{k}\right)} \tag{A69}$$

The minimum value ψ_m for the case of $k \in (0,1)$ is determined by the condition $E_{0,\mathrm{m}} = E_0(\psi_m) = k/e$ providing with Eq. (A65)

$$\psi_m = -\ln\left[\frac{ke^{\frac{1}{k}-1}}{1-\eta} - 1\right] \tag{A70}$$

Following the Appendix G.3 we can further reduce the inverse solution (A67) written as

$$\tau = \frac{1}{k}\int_{\psi_1}^{\psi_2} \frac{dx}{1 + W_{\mu}(-\frac{E_0(x)}{k})} = \frac{1}{k}\int_{z_0(\psi_1)}^{z_0(\psi_2)} \frac{dz_0}{(dz_0/dx)[1+W_{\mu}(z_0)]} \tag{A71}$$

Preprints (www.preprints.org) | NOT PEER-REVIEWED | Posted: 30 March 2021 doi:10.20944/preprints202103.0718.v1

with

$$\begin{aligned} z_0(x) &= -E_0(x)/k = -\frac{A(1+e^{-x})}{k}, \\ A &= (1-\eta)e^{-\frac{1}{k}} \end{aligned} \tag{A72}$$

Evaluating

$$\frac{dz_0}{dx} = \frac{Ae^{-x}}{k} = -\frac{A+kz_0}{k} \tag{A73}$$

then provides for Eq. (A71)

$$\tau = -\int_{z_0(\psi_1)}^{z_0(\psi_2)} \frac{dz_0}{(A+kz_0)[1+W_\mu(z_0)]} \tag{A74}$$

The substitution $z_0 = we^w$ then yields

$$\tau = \int_{W_\mu(z_0(\psi_2))}^{W_\mu(z_0(\psi_1))} \frac{dw}{kw + Ae^{-w}} \tag{A75}$$

which is still exact. With the substitution $y = e^{-w}$ the solution (A75) can be further rewritten. Integrals of this form have been approximated in Kröger and Schlickeiser [11].

Appendix G.3 SIV-case $b > 0$, $k = 0$

In the case of a negligible recovery rate $k = 0$ implying $\alpha = -b$ the Eq. (46) simplifies to

$$\Phi + b\ln\Phi - b\ln(1+e^{\psi}) = \Phi + b\ln\frac{\Phi}{1+e^{\psi}} = 1 + b\ln\eta, \tag{A76}$$

or with $\Phi = I_0 + S_0$ (we use the index 0 to indicate that we consider the limit $k = 0$ here) and Eq. (48)

$$I_0 + S_0 + b\ln I_0 = 1 + b\ln\eta_b \tag{A77}$$

Appendix G.3.1 Symmetry argument

By a simple symmetry argument the solution of Eq. (A77) can be expressed in terms of the SIR-function [11] G obeying Eq. (A58). Setting

$$I_0 = S,\ S_0 = I,\ b = -k,\ \eta_b = 1-\eta, \tag{A78}$$

Eq. (A77) becomes

$$I + S - k\ln S = 1 - k\ln(1-\eta), \tag{A79}$$

which is identical to Eq. (A56). Therefore we can use the SIR-function $G(\tau)$, obeying Eq. (A58), but now with negative values of k, to obtain for the SIV-solutions

$$\begin{aligned} S_0(\tau) &= \frac{dG}{d\tau}, \qquad I_0(\tau) = \frac{dG(\tau)}{d\tau}, \\ j(\tau) &= \frac{de^{-G}}{d\tau}, \qquad J(\tau) = 1 - e^{-G} \end{aligned} \tag{A80}$$

If one wants to follow this approach one has to calculate the function G for negative values of k.

Appendix G.3.2 Alternative inverse solution

For $k = 0$ one obtains $\alpha = -b$, so that Eq. (36) reads

$$\frac{d\psi}{d\tau} = -(b + \Phi) \tag{A81}$$

Preprints (www.preprints.org) | NOT PEER-REVIEWED | Posted: 30 March 2021 doi:10.20944/preprints202103.0718.v1

Likewise, the general solution (55) reduces to

$$\Phi = bW_0\left(\frac{E_b(\psi)}{b}\right) \tag{A82}$$

with the positive expression

$$E_b(\psi) = \eta e^{\frac{1}{b}}(1+e^{\psi}) \geq 0, \tag{A83}$$

As its argument is positive it has to be the principal Lambert function in Eq. (A82). Inserting the solution (A82) then provides for Eq. (A81)

$$\frac{d\psi}{d\tau} = -b\left[1+W_0\left(\frac{E_b(\psi)}{b}\right)\right], \tag{A84}$$

which with the initial condition (33) readily integrates to the inverse exact solution

$$-b\tau = \int_{\psi_0}^{\psi} \frac{dx}{1+W_0\left(\frac{E_b(x)}{b}\right)} \tag{A85}$$

Here also nearly all previous general results obtained in Sect. III and IV hold with α replaced by $-b$. With

$$z_b(x) = E_b(x)/b = \frac{1+e^x}{D}, \quad D = \frac{b}{\eta e^{\frac{1}{b}}}, \tag{A86}$$

implying

$$x = \ln(Dz_b - 1), \quad \frac{dx}{dz_b} = \frac{D}{Dz_b - 1} \tag{A87}$$

we find for Eq. (A85)

$$-b\tau = D\int_{\frac{1}{\eta D}}^{\frac{1+e^{\psi}}{D}} \frac{dz_b}{(Dz_b-1)[1+W_0(z_b)]} \tag{A88}$$

The substitution $z_b = we^w$ then yields

$$-b\tau = D\int_{W_0(\frac{1}{\eta D})}^{W_0(\frac{1+e^{\psi}}{D})} \frac{dw}{Dw - e^{-w}} \tag{A89}$$

which is still exact.

References

1. Estrada, E. Covid-19 and Sars-Cov-2. Modeling the present, looking at the future. *Phys. Rep.* **2020**, *869*, 1.
2. Kröger, M.; Schlickeiser, R. Forecast for the second Covid-19 wave based on the improved SIR-model with a constant ratio of recovery to infection rate. *Preprints* **2021**, p. 2021010449.
3. Schlickeiser, R.; Kröger, M. Analytical solution of the SIR-model for the temporal evolution of epidemics. Part B: Semi-time case. *J. Phys. A: Math. Theor.* **2021**, p. published online. doi 10.1088/1751-8121/abed66.
4. Morton, R.; Wickwire, K.H. On the optimal control of a deterministic epidemic. *Adv. Appl. Probab.* **1974**, *6*, 622–635.
5. Anderson, R.M.; May, R.M. *Infectious diseases of humans: dynamics and control*; Oxford Science Publications, Oxford, 1991.
6. Behncke, H. Optimal control of deterministic epidemics. *Optim. Control Appl. Methods* **2000**, *21*, 269–285.
7. Hansen, E.; Day, T. Optimal control of epidemics with limited resources. *J. Math. Biol.* **2011**, *62*, 423–451.
8. Grauer, J.; Löwen, H.; Liebchen, B. Strategic spatiotemporal vaccine distribution increases the survival rate in an infectious disease like Covid-19. *Sci. Rep.* **2021**, *10*, 21594.
9. Grundel, S.; Heyder, S.; Hotz, T.; Ritschel, T.K.S.; Sauerteig, P.; Worthmann, K. How to coordinate vaccination and social distancing to mitigate SARS-CoV-2 outbreaks. *medRxiv* **2020**, p. 2020.12.22.20248707.

10. Duclos, T.; Reichert, T. The missing Link: A closed form solution to the Kermack and Mckendrick epidemic model equations. *medRxiv* **2021**, p. 2021.03.02.21252781. doi:10.1101/2021.03.02.21252781.
11. Kröger, M.; Schlickeiser, R. Analytical solution of the SIR-model for the temporal evolution of epidemics. Part A: Time-independent reproduction factor. *J. Phys. A: Math. Theor.* **2020**, *53*, 505601.
12. Abramowitz, M.; Stegun, I.A. *Handbook of Mathematical Functions*; National Bureau of Standards, Washington, 1972.
13. Schüttler, J.; Schlickeiser, R.; Schlickeiser, F.; Kröger, M. Covid-19 predictions using a Gauss model, based on data from April 2. *Physics* **2020**, *2*, 197–212.
14. Kröger, M.; Schlickeiser, R. Gaussian doubling times and reproduction factors of the COVID-19 pandemic disease. *Frontiers Phys.* **2020**, *8*, 276.
15. 2021. Data repository https://github.com/owid/covid-19-data/blob/master/public/data/vaccinations/vaccinations.csv.
16. 2021. Data repository https://www.complexfluids.ethz.ch/cgi-bin/covid19-waveII.

 doi:10.20944/preprints202103.0718.v1

Ausführliche deutsche Zusammenfassung

6000 deutsche Covid-19 Tote zuviel durch zu langsames Impfen. Quantitative Modellierung der Covid-19 Epidemie mit Impfungen

Mit den seit Dezember 2020 verfügbaren und eingesetzten effektiven Impfstoffen gegen Covid-19-Infektion durch die Firmen Pfizer-BioNTech, Moderna und AstraZeneca ist es von grossen Interesse, deren Einfluss auf die zeitliche Entwicklung von Corona-Wellen quantitativ zu berechnen. Deshalb haben die Autoren das etablierte SIR-Schubladenmodell mit den drei Schubladen ansteckbar(S)-infiziert (I)-gesundet/verstorben(R) um die vierte Schublade geimpft (V) erweitert, und dabei die allgemein zeitabhängige Impfrate $v(t)$ als Transferrate von ansteckbar-zu-geimpft eingeführt. Die jeweiligen Werte von S, I, R und V in einer gegebenen homogenen Gesamtpopulation N bezeichnen die relativen Anteile von ansteckbaren, infizierten, gesundet/verstorbenen und geimpften Personen. In unterschiedlichen Ländern variiert die Impfrate deutlich: in Israel ist die Impfrate mit 0.007 pro Tag weltweit am höchsten, während sie in den EU-Ländern deutlich kleiner ist (in Deutschland 0.00042 pro Tag).

Beim Einfluss auf den zeitlichen Verlauf der Epidemie konkurriert die Impfrate v mit der Ansteckungsrate $a(t) \in [0.1 - 1.0]$ pro Tag und der Gesundet-Verstorben-Rate $\mu(t) = ka_0(t)$ pro Tag und $k \in [0.7 - 0.99]$, die insbesonders für die zweiten Corona-Wellen deutlich grösser sind. Ausbruchswellen treten nur dann auf, wenn die Summe von $k + b < 1 - 2\eta$ ist, wobei $b = v(0)/a(0)$ das Verhältnis von Impfrate zu Ansteckungsrate und η den Anteil der anfänglich beim Start der Welle infizierten und infizierenden Personen bezeichnen. Weil der Wert von η sehr klein gegen 1 ist, könnte man Ausbruchswellen komplett vermeiden, wenn das Verhältnis $b > 1 - k$ ist, d.h. wenn genügend viel geimpft wird, sodass die anfängliche Impfrate $v(0) > a(0) - \mu(0)$ grösser als die Differenz zwischen den anfänglichen Ansteckungs- und Gesundungs-Rate ist, was allerdings in keinem Land der Welt erreicht wurde.

In dieser Arbeit ist es den Autoren erstmalig gelungen, analytische Lösungen für die zeitliche Entwicklung aller relevanten Grössen $Q(t) \in [S(t), I(t); R(t), V(t), J(t), \dot{J}(t)]$ zu berechnen, wobei $\dot{J}(t) = a(t)S(t)I(t)$ und $J(t)$ die täglichen bzw. kumulativen Anteile von Neu-Infizierten angeben. Letztere Grössen sind medizinisch interessant, da sie den täglichen Bedarf $h(t) \simeq \dot{J}(t)/100$ an intensiv-medizinischer Behandlung und die Sterberate $d(t) \simeq \dot{J}(t)/200$ bestimmen. Bei der Berechnung der analytischen Lösungen wurde die zeitabhängige Infektionsrate $a(t)$ durch Einführung einer neuen reduzierten Zeitvariable τ eliminiert, die durch die Ableitung $d\tau/dt = a(t)$ definiert ist. Die analytischen Lösungen gelten dann für den Fall zeitlich konstanter Verhältnisse k und b zwischen Gesundet/Verstorben- bzw. Impf-Rate zur Infektionsrate. Analytische Lösungen haben wertvolle Vorteile gegenüber Lösungen in der Literatur, die durch numerische Integration der SIRV-Gleichungen erhalten wurden: erstens erlauben sie die eindeutige Identifikation der wichtigsten Parameter, die den Verlauf der Epidemiewelle bestimmen. Zweitens versteht man mit analytischen Lösungen die Korrelationen und gegenseitigen Abhängigkeiten aller relevanter Grössen. Und drittens sind sie wichtig zum Test eventueller zukünftiger numerischer Verfahren zur Epidemie-Entwicklung, die weitere komplizierende Effekte wie etwa Altersgruppen und nichthomogene räumliche Virus-Ausbreitung beinhalten. Bezüglich des ersten Vorteils zeigt sich in der Tat, dass die Werte der drei Parameter k, b und η komplett den Verlauf der Epidemiewelle in der reduzierten Zeit τ bestimmen; der Verlauf in realer Zeit t hängt dann zusätzlich noch von der vorgegebenen Zeitabhängigkeit der Infektionsrate $a(t)$ ab.

Die Autoren berechnen zunächst exakt sogenannte inverse Lösungen $\tau(Q)$ mit Hilfe von Lambert-Funktionen. Durch Invertierung der Lambert-Funktionen können mit hoher Genauigkeit die inversen Lösungen in die explizite Abhängigkeiten $Q(\tau)$ umgerechnet werden. Die Invertierung der Lambert-Funktionen funktioniert sehr gut für alle Werte von $b \geq b_c$, wobei b_c ein kleiner, aber endlicher kritischer Wert des Verhältnisses von anfänglicher Impf- zu Ansteckungsrate ist. Für kleine Werte von $b \in [0, b_c]$ werden die Lösungen durch lineare Interpolation der SIRV-Lösung bei b_c und der durch die Autoren in früheren Arbeiten berechneten exakten reinen SIR-Lösung mit $b = 0$ bestimmt. Diese Approximation funktioniert sehr gut, wie der Vergleich mit den numerisch berechneten exakten SIRV-Lösungen zeigt.

Der Einfluss von Impfungen auf den totalen kumulativen Anteil und die Maximalrate von Neu-Infizierten wird mit den aufgezeichneten Realdaten von Covid-19 während der zweiten Welle in verschiedenen Ländern untersucht. Dabei wird mit der tatsächlichen Impfrate die Reduktion in der Gesamtzahl der Infizierten bestimmt. Es zeigt sich, dass in Deutschland durch Impfungen insgesamt (aufsummiert über die Dauer der 2. Welle) 2.0 Millionen Personen weniger mit Covid-19 infiziert werden, was etwa 10000 vermiedenen Todesfällen entspricht. Durch eine hypothetisch angenommene verdoppelte Impfrate wird die Folge aus zu langsamer Impfrate abgeschätzt. In Deutschland hätte dies zu insgesamt 1.25 Millionen weniger infizierten Personen geführt, was etwa 6000 Todesfällen entspricht. Das zu langsame Impfen in Deutschland ist die Ursache für 6000 vermeidbare Covid-19 Todesfälle.

Eine Motivation für diese drastische deutsche Zusammenfassung ist der Wunsch der Autoren, dass ihre bedeutenden neuen Ergebnisse von den politisch Verantwortlichen in den Regierungen und den Medien erkannt und berücksichtigt werden. Wie an anderem Ort diskutiert, bestehen Zweifel daran, ob es in Deutschland eine dritte Welle gibt, da

 doi:10.20944/preprints202103.0718.v1

die täglichen Todesraten auch bei Berücksichtigung einer zeitlichen Retardierung nicht den Anstieg der durch Tests nachgewiesenen Neu-Infizierten wiedergeben. Die vorliegende Arbeit liefert eine Basis zur Beantwortung dieser Frage.